

NLOptControl: A modeling language for solving optimal control problems

Huckleberry Febbo, Paramsothy Jayakumar, Jeffrey L. Stein, and Tulga Ersal*

Abstract—Current direct-collocation-based optimal control software is either easy to use or fast, but not both. This is a major limitation for users that are trying to formulate complex optimal control problems (OCPs) for use in on-line applications. This paper introduces **NLOptControl**, an open-source modeling language that allows users to both easily formulate and quickly solve nonlinear OCPs using direct-collocation methods. To achieve these attributes, **NLOptControl** (1) is written in an efficient, dynamically-typed computing language called *Julia*, (2) extends an optimization modeling language called *JuMP* to provide a natural algebraic syntax for modeling nonlinear OCPs; and (3) uses reverse automatic differentiation with the acrylic-coloring method to exploit sparsity in the Hessian matrix. This work explores the novel design features of **NLOptControl** and compares its syntax and speed to those of *PROPT*. The syntax comparisons shows that **NLOptControl** models OCPs more concisely than *PROPT*. The speeds of various collocation methods within *PROPT* and **NLOptControl** are benchmarked over a range of collocation points using performance profiles; overall, **NLOptControl**'s single, two, and four interval pseudospectral methods are roughly 14, 26, and 36 times faster than *PROPT*'s, respectively. **NLOptControl** is well-suited to improve existing off-line and on-line control systems and to engender new ones.

I. INTRODUCTION

Optimal control software packages that implement direct-collocation methods are used in a number of off-line [1], [2], [3], [4], [5], [6] and on-line [7], [8] applications as summarized in Table I. The primary function of these packages is to directly transcribe a human modeler's formulation of an optimal control problem (OCP) into a nonlinear programming problem (NLP). A key challenge with this process is enabling human modelers (i.e., users) to easily formulate new and complex problems while producing an NLP that can be quickly solved by an external NLP solver. However, current direct-collocation-based optimal control software packages are generally either fast or easy to use, but not both. Thus, these package are not well suited for non-expert users trying to formulate complex problems for on-line applications, wherein speed is critical. Therefore, there is a need for a direct-collocation-based optimal control software package that is both fast and easy to use. In this paper, an approach to bridging this gap

The authors wish to acknowledge the financial support of the Automotive Research Center (ARC) in accordance with Cooperative Agreement W56HZV-14-2-0001 U.S. Army Tank Automotive Research, Development and Engineering Center (TARDEC) Warren, MI., DISTRIBUTION A. Approved for public release; distribution unlimited.

H. Febbo, J. L. Stein, and T. Ersal are with the Department of Mechanical Engineering, University of Michigan, Ann Arbor, MI 48109 USA (e-mail: febbo@umich.edu; stein@umich.edu; tersal@umich.edu).

P. Jayakumar is with the U.S. Army RDECOM-TARDEC, Warren, MI 48397 (email: paramsothy.jayakumar.civ@mail.mil)

*Corresponding author (tersal@umich.edu)

Software	Applications						Properties		
	Off-line			On-line			Open-source	Easy to use	Fast
	Chemical	Space vehicle	Medical	Air vehicle	Ground vehicle	Robot			
<i>GPOPS-ii</i>	[1]	[1], [2]				[17]†	x	✓	x
<i>PROPT</i>	[3]	[3]	[3]				x	✓	x
<i>GPOCS</i>		[4]		[18]†			x	✓	x
<i>DIDO</i>		[5]		[18]†			x	✓	x
<i>ACADO</i>					[8]		✓	x	✓
<i>CasADi</i>	[6]					[7]	✓	x	✓
Custom					[19], [20]†		x	x	x
NLOptControl					[9]		✓	✓	✓

TABLE I: Landscape of direct-collocation-based optimal control software focusing on their applications and properties. † indicates that the software is too slow for use the on-line application.

is presented and incorporated into a new, open-source optimal control modeling language called **NLOptControl** [9].

As seen in Table I, some of the most well-known optimal control software packages (*GPOPS-ii*, *PROPT*, *DIDO*) are closed-source and often require a licensing-fee. These drawbacks limit their research value, since they are not freely available to the entire research community, results may be difficult to reproduce, and if the details of the underlying algorithms cannot both be seen and modified, then open validation and development of these algorithms is not possible [10], [11]. Fortunately, several noteworthy open-source optimal control software packages exist. For completeness, this paper does not limit its discussions to these open-source packages.

Optimal control packages with an algebraic syntax that closely resembles the Bolza form of OCPs [12] are categorized as easy to use. It is noted that there are other design features that affect ease of use; for instance, not having a built-in initialization algorithm [13] reduces ease of use, but these aspects of ease of use are not addressed in this paper. Table I shows that this work categorizes the direct-collocation-based optimal control software packages *GPOPS-ii* [1], *PROPT* [3] and *GPOCS* [14] as easy to use and *CasADi* [15] and *DIDO* [16] as not easy to use.

For ease of use, modeling languages should have a syntax that closely resembles the class of problems for which they have been designed. Modeling languages like AMPL and GAMS are not embedded in a pre-existing computational language, which allows for syntactical flexibility, when developing them. However, this approach (1) makes development of the modeling language difficult and time-consuming, and (2) does not directly expose users to the breath of features avail-

able in a computational language such as *C++* or *MATLAB*. For these reasons, modeling languages are often embedded in a pre-existing computational language.

It can be difficult to establish a syntax for the modeling within the syntactical confines of a pre-existing computational language. To overcome this issue, operator overloading can be used. For instance, a multiple-shooting method based optimal control software package called *ACADO* [21] uses operator overloading to allow its user to define an OCP using symbolic expressions that closely resemble the actual mathematical expressions of the problem. However, a naive implementation of operator overloading can lead to performance issues [22]. Additionally, Moritz Diehl, a researcher who developed *ACADO* and *MUSCOD-II*, later acknowledges that, *ACADO* Toolkit [21], *DIRCOL* [23], *DyOS* [24], and *MUSCOD-II* [25] restrict the problem formulations, particularly for users not involved with the development of these tools [15]. The above acknowledgment is included in a paper [15] that introduces *CasADi*. *CasADi* allows users to formulate OCPs with fewer restrictions than *ACADO*. However, *CasADi* requires that users write the code for the transcription methods. Transcription methods are a general class of numerical methods used to approximate continuous-time OCPs; a direct-collocation method is a type of transcription method. *CasADi* lets users to code their own transcription methods to avoid creating a "black box" OCP solver that is only capable of solving restrictive formulations, as with *ACADO*. While this approach may be pedagogically valuable for users, it can lead to bugs and long development time [26] and it makes *CasADi*'s syntax not closely resemble OCPs. For these reasons, this paper does not categorize *CasADi* as easy to use. On similar grounds, *DIDO* is not categorized as easy to use.

For safety in on-line applications, the trajectory needs to be provided to the plant in real-time. An on-line optimal control example is a nonlinear model predictive control (NMPC) problem. Real-time is achieved when the NLP solve-times are all less than the chosen execution horizon. Otherwise, the low-level controllers will not have a trajectory to follow. Despite the need for small solve-times (i.e., speed), several implementations of direct-collocation methods within the *MATLAB* computational language are not able to achieve solve-times that are less than the execution horizon for a number of NMPC applications. As seen in Table I, *GPOCS*, *GPOPS-ii*, and custom *MATLAB* software are not fast enough for NMPC applications in aircraft [18], robot [17], and UGV [19], [20] systems, respectively. On the other hand, *CasADi*, which is written in *C++*, is fast enough for an NMPC application in a robot system [7]. Given this practical limitation, this paper will now discuss why some direct-collocation-based optimal control packages are fast while others are slow.

As seen in Table I, this work categorizes *GPOPS-ii*, *PROPT*, *GPOCS*, and *DIDO* as slow and *CasADi* as fast. If a package uses sparse automatic differentiation methods implemented in a computation language that approaches the speeds of *C*, it is categorized as fast; the reasoning for this categorization is explained below.

The main algorithmic step in direct method based numerical optimal control is solving the NLP. The solve-time for this

step consists of two major parts: (1) the time spent running optimization algorithms within the NLP solver, and (2) the time spent evaluating the nonlinear functions and their corresponding derivatives. Fortunately, low-level algorithms, which are available within several prominent NLP solvers, such as *KNITRO* [27], *IPOPT* [28], and *SNOPT* [29], can be used to reduce the time associated with running the optimization algorithms. The second component is discussed here in terms of current direct-collocation-based optimal control software packages.

The speed of direct-method-based optimal control software depends on the speed of the differentiation method within the computational language in which it is implemented. *GPOPS-ii* uses a sparse finite difference method [30] to calculate the derivatives using the *MATLAB* computational language. However, finite difference methods, like the sparse finite difference method, are not only slow, but they are also inaccurate [31]. In addition to this, the dynamically-typed *MATLAB* computational language is typically slow in comparison to statically-compiled languages such as *C* and *Fortran*. Since *GPOPS-ii* uses a slow differentiation method within a relatively slow computational language, it is categorized as slow. *PROPT* uses either symbolic- or forward-automatic differentiation to calculate the derivatives using *MATLAB*. While *PROPT*'s methods are more accurate and generally faster than finite difference methods, they do not exploit the sparse structure of the Hessian matrices that is born from a direct-collocation method, like the sparse finite difference method in *GPOPS-ii*. Given this computational limitation and the slow speed of *MATLAB*, this paper considers *PROPT* to be slow as well. On the other hand, *CasADi* uses the star-coloring method [32] to exploit the sparse structure of the Hessian matrix and reverse automatic differentiation implemented in *C++* [15]. Since *CasADi* employs a differentiation methods that is well suited for the sparse structure of the Hessian matrix and it is implemented in a fast computational language, *CasADi* is categorized as fast. On similar grounds, this paper identifies *GPOCS* and *DIDO* as slow.

In sum, there is no direct-collocation-based optimal control software package is both fast and easy to use. *CasADi* is fast, but not easy to use; and *GPOPS-ii*, *PROPT*, and *GPOCS* are easy to use, but not fast. Thus, there is a need for a package that is both fast and easy to use.

This paper investigates an approach for improving both speed and ease of use of optimal control software. As described in detail in Section II, this approach uses recent advances in computational languages and differentiation methods in contrast to the computational languages and differentiation methods used by current direct-collocation-based optimal control software. Additionally, also unlike current direct-collocation-based optimal control software packages, this approach extends an optimization modeling language to include syntax for modeling OCPs. More specifically, this approach is as follows:

Approach

- For ease of use and speed, `NLOptControl` is embedded in the fast, dynamically-typed *Julia* programming lan-

guage [33].

- For increased ease of use, `NLOptControl` extends the `JuMP` optimization modeling language [34], which is written in *Julia*, to include a natural syntax for modeling OCPs in Bolza form.
- For increased speed, `NLOptControl` uses the acrylic-coloring method [35] to exploit sparsity in the Hessian matrix and reverse-automatic differentiation through the `ReverseDiff` package [36], which is also written in *Julia*.

Therefore, this work addresses the following research question: Can the above outlined approach improve speed and ease of use of direct-collocation-based optimal control software? This question is answered by comparing `NLOptControl`'s speed and ease of use to those of *PROPT*.

`NLOptControl` was released as a free, open-source software package in the summer of 2017 [9]. Since then, the literature has shown that `NLOptControl` is fast and easy to use. For speed, `NLOptControl` was leveraged to solve complex trajectory planning problems for an unmanned ground vehicle system in real-time — solving these types of problems in real-time using *MATLAB* was not feasible in prior work [19], [20]. For ease of use, `NLOptControl` was used to create a new optimal control based learning algorithm [37] without any help from the developers of `NLOptControl`.

The remainder of this paper is organized as follows. Section II further describes `NLOptControl`'s approach to bridging the research gap. Section III describes the classes of off-line and on-line OCPs that can be solved using `NLOptControl`. Section IV provides a brief background on numerical optimal control and a mathematical description of the direct-collocation methods implemented within `NLOptControl`. Section VI provides an example that compares `NLOptControl`'s ease of use against *PROPT*'s and benchmarks `NLOptControl`'s speed against *PROPT*. Section VII answers the research question and discusses further implications. Finally, Section VIII summarizes the work and draws conclusions.

II. SOFTWARE ECOSYSTEM

Advances in computational languages, optimization modeling languages, and differentiation methods and tools made it possible to create `NLOptControl`. This section describes these software advances and shows how they can be leveraged to create a modeling language for a class of optimization problems.

A. Computational languages

Direct-collocation based optimal control software packages are embedded in either a statically- or a dynamically typed computational language. Dynamically typed languages enable users to quickly develop and explore new concepts, yet they are typically slow; statically typed languages sacrifice the user's productivity for speed. Recently, however, a dynamically typed computing language called *Julia* has become a popular alternative to the computing languages that the current optimal control software packages are embedded in. It has become popular, because it allows users to write high-level

code that closely resembles their mathematical formulas, while producing low-level machine code that approaches the speed of *C* and is often faster than *Fortran* [33]. The claim that *Julia* is not only fast, but also easy to use, motivates the investigation presented in this paper. Specifically, this paper investigates the ability of the *Julia* computational language to improve speed and ease of use for optimal control software.

B. Modeling optimization problems

In the late 1970's, researchers using optimization software were more concerned with the need to improve the software's ease of use than its speed [38]. Eventually, this concern led to the development a number of optimization modeling languages, such as *GAMS* [39] and *AMPL* [40]. The role of an optimization modeling language is to translate optimization problems from a human-friendly language to a solver-friendly language [41], [42]. In other words, optimization modeling languages do not solve optimization problems; they focus on modeling problems at a high-level and passing optimization problems to external low-level solvers, which are the NLP solvers and the differentiation tools in the context of this work. Similarly, in this work, the high-level problem is the NLP, given in Eqn. 1 - Eqn. 3 (i.e., the NLP model) as

$$\underset{z \in \mathbb{R}^n}{\text{minimize}} \quad f(z) \quad (1)$$

$$\text{subject to} \quad g(z) \leq 0 \quad (2)$$

$$h(z) = 0 \quad (3)$$

where the objective function $f : \mathbb{R}^n \rightarrow \mathbb{R}$, with n defined as the number of design variables; the inequality constraints $g : \mathbb{R}^n \rightarrow \mathbb{R}^e$; and the equality constraints $h : \mathbb{R}^n \rightarrow \mathbb{R}^q$, are all assumed to be twice-continuously differentiable functions [28], [43].

A number of standard optimization problem classes do not fit readily into the NLP model. In addition to this, translating these standard problem classes into the NLP model can require significant work. Thus, for users interested in simply modeling these standard problem classes, and not translating these problems into an NLP model, the NLP model should be extended to include higher-level modeling languages for these standard problem classes. However, most optimization modeling languages are not designed to be extended in this fashion [42]. Because of this limitation, both the speed and ease of use of optimal control packages have suffered. *GPOCS*, *GPOPS-ii*, and *PROPT* are slow because the sparse-automatic differentiation methods — typically available through an optimization modeling language — are not available in *MATLAB*; so, these packages use less efficient differentiation methods. Additionally, since these packages are not built upon an existing NLP modeling language, the API tends to be overly flexible, which can lead to modeling errors [21].

JuMP [22], a recent optimization modeling language that is embedded in the fast, dynamically-typed *Julia* programming language [33], is designed to be extended to include new classes of optimization problems. *JuMP* extensions include: parallel multistage stochastic programming [44], robust optimization [45], chance constraints [46], and sum of squares

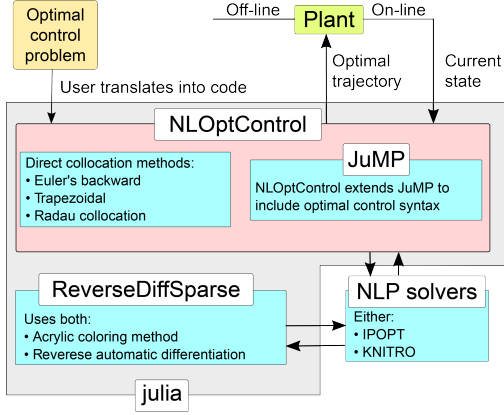


Fig. 1: Proposed software framework for nonlinear OCPs.

[47]. Moreover, *JuMP* provides an interface for both the *KNITRO* and *IPOPT* NLP solvers as well the *ReverseDiff* differentiation tool. *ReverseDiff* [36] is also embedded in the *Julia* programming language and utilizes reverse automatic differentiation with the acrylic-coloring method [48] to exploit sparsity in the Hessian matrices. Research shows that the acrylic-coloring method is faster than the star-coloring method [48], which was used in the *CasADi* package [15]. These advances are leveraged to create an optimal control modeling language called *NLOptControl*.

C. Proposed software ecosystem

Fig. 1 presents *NLOptControl*'s software ecosystem and its function as an optimal control software package. In terms of this ecosystem, it is: embedded in *Julia*; extends *JuMP* to provide a natural syntax for modeling OCPs; leverages *ReverseDiff*; and interfaces with *KNITRO*, *IPOPT*, and potentially other solvers to solve the automatically formulated NLP problem. To use *NLOptControl*, users need only formulate their OCP into a syntax-based model of the OCP. This model is then approximated using one of the direct-collocation methods implemented in *NLOptControl*, which at the time of this writing include: the Euler's backwards, the trapezoidal, and the Radau collocation methods. After the model has been approximated, the software ecosystem solves this approximation to determine an optimal trajectory. This trajectory can then be followed using low-level controllers to control the plant for either an off-line or on-line tasks.

III. SCOPE OF *NLOptControl*

NLOptControl is designed for modeling OCPs and solving them for either off-line or on-line applications. This section shows the types of problems that *NLOptControl* can model, and demonstrates *NLOptControl*'s visualization capabilities and salient design features for on-line applications (e.g., NMPC problems).

A. Modeling OCPs

An important class of optimization problems is the OCP. *NLOptControl* models single-phase, continuous-time, OCP

in a Bolza form [12] that is tailored for NMPC problems and adds slack constraints on the initial and terminal states as

$$\begin{aligned} & \underset{x(t), u(t), x_{0s}, x_{fs}, t_f}{\text{minimize}} && \mathcal{M}(x(t_0 + t_{ex}), t_0 + t_{ex}, x(t_f), t_f) \\ & && + \int_{t_0 + t_{ex}}^{t_f} L(x(t), u(t), t) dt \\ & && + w_{s0}x_{0s} + w_{sf}x_{fs} \end{aligned} \quad (4)$$

$$\text{subject to} \quad \frac{dx}{dt}(t) - F(x(t), u(t), t) = 0 \quad (5)$$

$$C(x(t), u(t), t) \leq 0 \quad (6)$$

$$x_0 - x_{0_{tol}} \leq x(t_0 + t_{ex}) \leq x_0 + x_{0_{tol}} \quad (7)$$

$$x_f - x_{f_{tol}} \leq x(t_f) \leq x_f + x_{f_{tol}} \quad (8)$$

$$x_{min} \leq x(t) \leq x_{max} \quad (9)$$

$$u_{min} \leq u(t) \leq u_{max} \quad (10)$$

$$t_{f_{min}} \leq t_f \leq t_{f_{max}} \quad (11)$$

$$x_0 - x(t_0 + t_{ex}) \leq x_{0s} \quad (12)$$

$$x_0 + x(t_0 + t_{ex}) \geq x_{0s} \quad (13)$$

$$x_f - x(t_f) \leq x_{fs} \quad (14)$$

$$x_f + x(t_f) \geq x_{fs} \quad (15)$$

where t_0 is the fixed initial time, t_{ex} is the fixed execution horizon that is added to account for the non-negligible solve-times in NMPC applications, t_f is the free final time, t is the time, $x(t) \in \mathbb{R}^{n_{st}}$ is the state, with n_{st} defined as the number of states, and $u(t) \in \mathbb{R}^{n_{ctr}}$ is the control, with n_{ctr} as the number of controls. $x_{s0} \in \mathbb{R}^{n_{st}}$ and $x_{sf} \in \mathbb{R}^{n_{st}}$ are optional slack variables for the initial and terminal states, respectively. The objective functional includes $\mathcal{M} : \mathbb{R}^{n_{st}} \times \mathbb{R} \times \mathbb{R}^{n_{st}} \times \mathbb{R} \rightarrow \mathbb{R}$ and $L : \mathbb{R}^{n_{st}} \times \mathbb{R}^{n_{ctr}} \times \mathbb{R} \rightarrow \mathbb{R}$, which are the Mayer and Lagrangian terms, respectively. Here $w_{s0}x_{0s} + w_{sf}x_{fs}$ is added to the Bolza form to accommodate slack variables on the initial and terminal conditions; this term is described in detail later in this section. $x_{0s} \in \mathbb{R}^{n_{st}}$ and $x_{fs} \in \mathbb{R}^{n_{st}}$ are vectors of weight terms on the slack variables for the initial and final state constraints. $F : \mathbb{R}^{n_{st}} \times \mathbb{R}^{n_{ctr}} \times \mathbb{R} \rightarrow \mathbb{R}^{n_{st}}$ and $C : \mathbb{R}^{n_{st}} \times \mathbb{R}^{n_{ctr}} \times \mathbb{R} \rightarrow \mathbb{R}^p$ denote the dynamic constraints and the path constraints, respectively; p is the number of path constraints. $x_0 \in \mathbb{R}^{n_{st}}$ and $x_f \in \mathbb{R}^{n_{st}}$ denote the desired initial and final states, respectively. $x_{0_{tol}} \in \mathbb{R}^{n_{st}}$ and $x_{f_{tol}} \in \mathbb{R}^{n_{st}}$ establish tolerances on the initial and final state, respectively. Constant upper and lower bounds on the state, control, and final time are included with Eqn. 9, Eqn. 10, and Eqn. 11, respectively. Finally, *NLOptControl* adds Eqn. III-A - Eqn.

III-A to the Bolza form for optional slack constraints on the initial and terminal states.

`NLOptControl` is embedded in the *Julia* language and specializes *JuMP*'s syntax to better suit the domain of optimal control. *JuMP* leverages *Julia*'s syntactic macros [33] to enable a natural algebraic syntax for modeling optimization problems, without sacrificing performance or restricting problem formulations [22]. `NLOptControl` extends *JuMP* to include syntax for modeling OCPs in Boltza form in Eqn. 4 – Eqn. 11, with the option of including slack constraints on the initial and terminal states through Eqn. – Eqn. .

For a basic example of this syntax, `NLOptControl` is now used to model the Bryson-Denham problem, which is given in mathematical form as

$$\begin{aligned} & \underset{a(t)}{\text{minimize}} && \frac{1}{2} \int_0^1 a(t)^2 dt \\ & \text{subject to} && \\ & \dot{v}(t) = a(t), & \dot{x}(t) = v(t), & x(t) \leq \frac{1}{12} \\ & v(0) = -v(1) = 1, x(0) = & x(1) = 0 \end{aligned}$$

The `define()` function is used to create a model object and define Eqn. 7 - Eqn. 10 as

```
n = define(numStates = 2, numControls = 1, X0
  ↪ = [0., 1.], XF = [0., -1.], XL = [0., NaN],
  ↪ XU = [1/12, NaN], CL = [NaN, NaN], CU = [
  ↪ NaN, NaN])
```

where `n` is an object that holds the entire optimal control model, `numStates` and `numControls` are the number of states and controls, `X0` and `XF` are arrays of the initial and final state constraint, `XL` and `XU` are arrays of any lower and upper state bounds, `NaN` indicates that a particular constraint is not applied, and `CL` and `CU` are an arrays of any lower and upper control bounds.

The dynamic constraints in Eqn. 5 are then added to the model through the `dynamics` function as

```
dynamics!(n, [: (x2[j]), : (u1[j])])
```

where the `!` character indicates that the model object `n` is being modified by the function. The elements of the array `:(x2[j] ↪)` and `:(u1[j])` represent $v(t)$ and $a(t)$; by default the state and control variables are `x1, x2, . . .` and `u1, u2, . . .`, but they can be changed. Differential equations must be passed within an array of *Julia* expressions (i.e., `[: (), : (), . . . , : () ↪]`), and the index `[j]` must be appended to the state and control variables. `j` is used within `NLOptControl` to index particular time discretization points $\in [t_0 + t_{ex}, t_f]$.

The next step is to indicate whether or not the final time t_f is a design variable using the `configure` function as

```
configure!(n; (:finalTimeDV => true))
```

where `(:finalTimeDV=>true)` indicates that the final time is a design variable, which is the case for the Bryson-Denham problem. Additional options can be passed to the `configure` function. However, this paper is not a tutorial; for a tutorial see `NLOptControl`'s documentation [9].

At this point, any path constraints in Eqn. 6 can be added to the model using *JuMP*'s `@NLconstraint` macro. However, these constraints are not needed for this example.

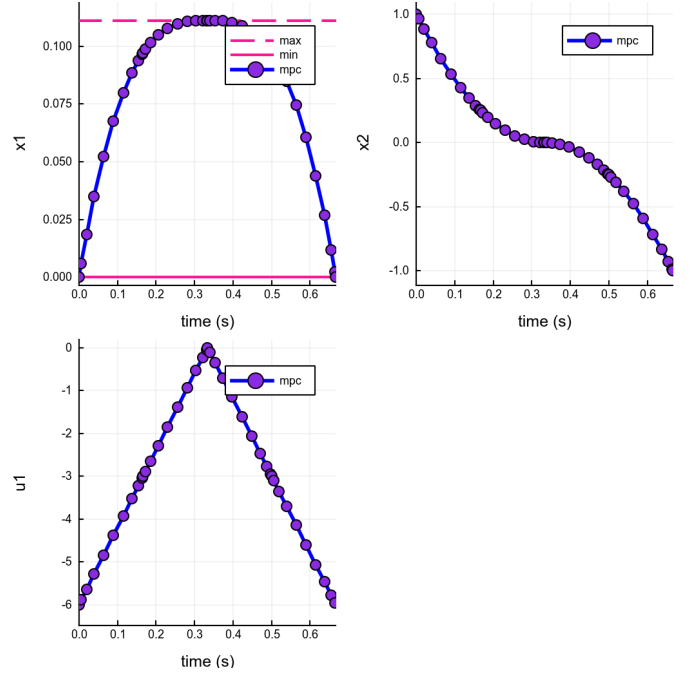


Fig. 2: Output of `allPlots(n)` command after modeling and solving the Bryson-Denham problem using `NLOptControl`. Section A in the Appendices provides additional plots of the `NLOptControl`'s solution to the Bryson-Denham problem compared to the analytical solution, including the costates.

Next, the objective function in Eqn. 4 is added to the model. To accommodate for a Lagrangian term, `NLOptControl` provides the `integrate` function—similar to the `dynamics` function, an expression must be passed and the `[j]` syntax must be appended to all state and control variables. For the Bryson-Denham, the objective functional is modeled as

```
obj = integrate!(n, :(0.5*u1[j]^2))
```

The *JuMP* macro `@NLobjective` is used to add the objective functional to the model as `@NLobjective(n.ocp.mdl, Min ↪ , obj)`. This problem is solved by passing the model `n` to the `optimize` function as

```
optimize!(n)
```

a) *Visualization*: `NLOptControl` allows users quickly plot the solutions to their problems. For plotting —by default— `NLOptControl` leverages *GR* [49] as a backend, but it can be configured to utilize *matplotlib* [50] instead. The command `allPlots(n)` plots the solution trajectories for the states, controls, and costates¹. Invoking this command to visualize the solution to the Bryson-Denham problem that is modeled above produces Fig. 2.

B. Nonlinear model predictive control

Fig. 3 depicts two ways that `NLOptControl` can be used to solve OCPs for NMPC applications; Fig. 3a neglects control delays and Fig. 3b accounts for them. This section

¹if `n.s.ocp.evalCostates` is set to `true`

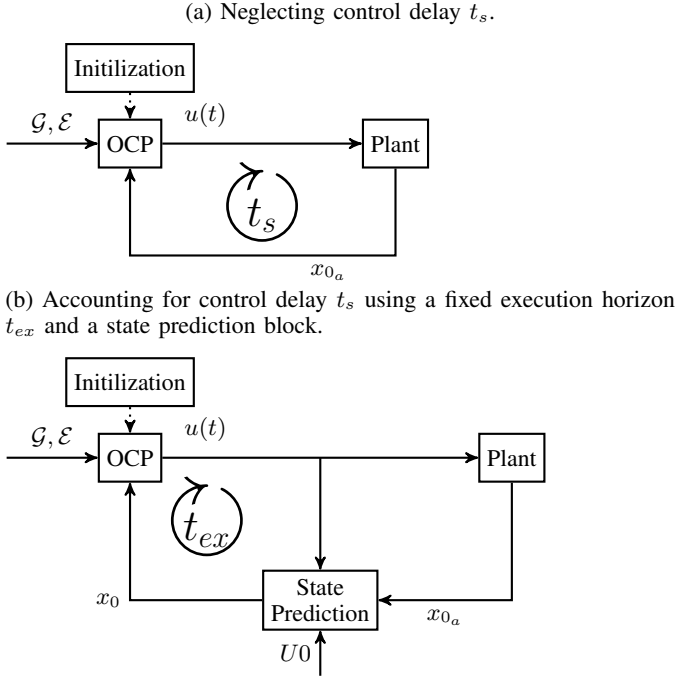


Fig. 3: Nonlinear model predictive control framework available in `NLOptControl`.

describes these figures and discusses the design features that help `NLOptControl` users tackle NMPC problems.

Fig. 3a has three main components: the OCP, the plant, and the initialization block. Three inputs \mathcal{G} , \mathcal{E} , and x_0 are provided to the OCP to produce $u(t)$; $u(t)$ can be either a reference trajectory or control signals for the plant. In the case that $u(t)$ is a reference trajectory, then low-level controllers are added to the plant to allow it to track the trajectory.

Description: III.1. *Goal information \mathcal{G} includes the final desired state of the plant, which may not be equal to x_f . For instance, in an automated vehicle trajectory planning system, the goal range may be outside of the sensing range. In this case, the final desired state x_f may be near the boundary of the sensing range.*

Description: III.2. *Environment information \mathcal{E} includes any transient data. For example, this data may include the obstacle data that helps establish the constraints on obstacle avoidance for automated vehicle navigation problems.*

The plant can be either physical or virtual, but in either case is provided by the user. Because time can typically be allocated to initialize NMPC problems, the initialization block permits users to warm start their optimization problems so that the initial on-line solve time is much smaller. After initialization, at t_0 , the first control signal $u(t)$ is sent to the plant and the first on-line OCP is solved. Each time an OCP-solve starts, t_0 is reset to the current time. An issue with this scheme is that it does not take into account the solve time (i.e., control delay t_s). That is, the initial state of the OCP is constrained to be the current state of the plant x_0 at the initial time t_0 , so by the time the OCP has been solved t_s has elapsed, and the plant will have evolved to a new state. If this control delay is small

relative to the time scale of the dynamics, then neglecting it will not compromise the robustness. However, if the control delay is relatively large, then it cannot be neglected.

Fig. 3b illustrates an approach that accounts for these control delays. This approach adds a block that predicts the plant state at the current time plus a fixed execution horizon $t_0 + t_{ex}$. The execution horizon t_{ex} can be chosen based on the a heuristic upper limit on the solve times; often solve times do not change drastically when solved in a receding-horizon with varying parameters for the initial conditions and path constraints. This approach avoids having to predict individual solve times t_s .

`NLOptControl` provides various functionality tailored for solving NMPC problems. The remainder of this section simultaneously describes these features and provides an example that uses `NLOptControl` to formulate an OCP and solve it in a receding horizon. To this end, consider the moon lander OCP [51], which is given in without slack constraints in Eqn. 16 as

$$\begin{aligned}
 & \underset{a(t), t_f}{\text{minimize}} && \int_0^{t_f} a(t) dt \\
 & \text{subject to} && \dot{x}(t) = v(t), \quad \dot{v}(t) = a(t) - g \\
 & && x(t_0) = 10, \quad x(t_f) = 0 \\
 & && v(t_0) = -2, \quad v(t_f) = 0 \\
 & && 0 \leq x(t) \leq 20, \quad -20 \leq v(t) \leq 20 \\
 & && 0 \leq a(t) \leq 3, \quad 0.001 \leq t_f \leq 400
 \end{aligned} \tag{16}$$

where the $x(t)$ is the altitude, $v(t)$ is the speed, $a(t)$ is the thrust, $g = 1.5$ is the local gravitational acceleration, t_f is the final time. The objective is to minimize the thrust of the spaceship given the dynamic constraints, event constraints, control constraints, and final time constraints. Listing. 1 shows the code needed to solve Eqn. 16 as an MPC problem. Line 1 creates a model `n` of the OCP with the initial and terminal state constraints, and the constant upper and lower bounds on the state and control variables. As is, the model `n` has low-tolerance hard constraints on the initial and terminal state conditions. However, these low-tolerance hard constraints can lead to infeasible problems and longer solve-times, especially when the loop is closed. That is, when the control drives the plant into an infeasible state space, an infeasible problem is engendered [52]; and typically, the solve-times increase as the problems become less-feasible. Therefore, an ability to easily adjust these low-tolerance constraints to high-tolerance hard constraints is desirable. As seen in Line 2, `NLOptControl` enables this feature through the `defineTolerances` function. `X0_tol` and `XF_tol` are arrays that set the tolerances on the initial $x_{0_{tol}}$ and final states $x_{f_{tol}}$, respectively.

When going from low- to high-tolerance hard constraints on the initial and terminal states, slack constraints should also be added. Because, when using these high-tolerance constraints without slack constraints, there is nothing pushing the initial and terminal states away from the edge of the infeasible region. Thus, infeasible problems are just as likely to occur. Adding slack constraints on the initial and terminal state constraints helps to mitigate these infeasible problems. Before slack constraints are added to the model, slack variables must

Listing 1: `NLOptControl` code needed to formulate and solve the moon lander as an MPC problem.

```

n = define(numStates = 2, numControls = 1, X0 = [10., -2], XF = [0., 0.], CL = [0.], CU = [3.])
2 defineTolerances!(n; X0_tol = [0.01, 0.005], XF_tol = [0.01, 0.005])
dynamics!(n, [(x2[j]), (u1[j]-1.5)])
4 configure!(n; (:finalTimeDV => true), (:xFslackVariables => true), (:x0slackVariables => true))
obj = integrate!(n, (u1[j]))
6 @NObjective(n.ocp.mdl, Min, obj + 100*(n.ocp.x0s[1] + n.ocp.x0s[2] + n.ocp.xFs[1] + n.ocp.xFs
↪ [2]))
initOpt!(n)
8 defineMPC!(n; tex = 0.2, predictX0 = true)
function IPplant(n, x0, t, U, t0, tf)
10 spU = linearSpline(t, U[:,1])
f = (dx, x, p, t) -> begin
12 dx[1] = x[2]
dx[2] = spU[t] - 1.5
14 end
return DiffEqBase.solve(ODEProblem(f, x0, (t0, tf)), Tsit5()), [spU]
16 end
defineIP!(n, IPplant)
18 simMPC!(n)

```

be added. The size of a slack variable corresponds to the size of the respective constraint violation [53]. As seen in Line 4, `NLOptControl` allows such slack variable to be added using the `configure` function. `(:xFslackVariables ↪ =>true)` and `(:x0slackVariables=>true)` adds slack variables on the initial and final state constraint, respectively. Both the objective of the moon lander problem and the slack constraints are added to model as on Line 6. `n.ocp.x0s` and `n ↪ .ocp.xFs` are arrays holding the slack variables on the initial and terminal states, respectively, and all of the terms in w_{s0} and w_{sf} (in Eqn. 4) are set to 100—these weights are set large enough such that the respective constraint violations are nearly zero. On Line 7, `NLOptControl` warm starts the optimization using the `initOpt` function; the initialization block in Fig. 3 captures this step.

The `defineMPC` function adds several basic settings to the model `n`. `tex` is the value of the fixed execution horizon and `predictX0` is a bool, which, when set to `true`, indicates that the the framework in Fig. 3b is used. Thus, a prediction of the initial state needs to be made either by the user or using an internal model of the plant, which is added to `n`. In this simple example, the differential equations in Eqn. 16 govern the OCP, the plant, and the state prediction function. The plant and prediction model are defined by the `IPplant` function from Line 9 to Line 16 and passed to the model `n` using the `defineIP` function on Line 17. Here the `IPplant` function is showed for completeness, but its is not described in detail since it uses the well-documented *DifferentialEquations* package in *Julia* [54]. For safety and reduced time in experimental development, this initial step, i.e., making all of the models the same and running a simulation-based experiment, should be taken; especially when formulating more complex OCPs for practical NMPC applications.

a) Visualization: The command `mcpPlots(n,idx)` plots the data for both plant and solution trajectories for the states and controls, the predicted initial state, and the optimization times, where `idx` is an integer representing the iteration

number. For instance, invoking this command to visualize data at the 4th and 15th iterations of the moon lander problem produces Fig. 4a and Fig. 4b, respectively; `NLOptControl` provides visualization functionality to combine the frames from all iterations into a single animation.

Section B-A in the Appendices provides a plot `NLOptControl`'s closed-loop solution to the moon lander problem compared to the analytical solution.

IV. NUMERICAL OPTIMAL CONTROL

This section provides an overview of numerical optimal control methods (i.e., transcription methods). The goal of this section is to motivate the choice of direct-collocation methods in `NLOptControl`, not to provide the reader with a complete description of numerical optimal control methods. Readers are referred to [55], [56], [43], for more comprehensive reviews on this subject. After these methods are discussed, the mathematics of the various direct-collocation methods as they are implemented in `NLOptControl` are provided.

A. Numerical optimal control overview

Tractable exact algorithms for solving OCPs suitable for practical applications do not exist; thus, numerical methods are used [57]. Numerical methods for solving OCPs (i.e., trajectory optimization problems) are generally broken into two categories: indirect and direct methods. Indirect methods seek the root of the necessary conditions for optimality [58] while direct methods seek the extrema of the cost functional [55]. Compared to direct methods, indirect methods produce better error estimates [12] and require less preliminary work to determine optimality [59]. However, indirect methods have several disadvantages: the necessary conditions must be derived [60]; the incorporation of path constraints requires an a priori estimation of the sequence of constrained/unconstrained singular arcs; and a guess needs to be made for the adjoint variables [43]. Due to these disadvantages, `NLOptControl` solves OCPs using direct methods.

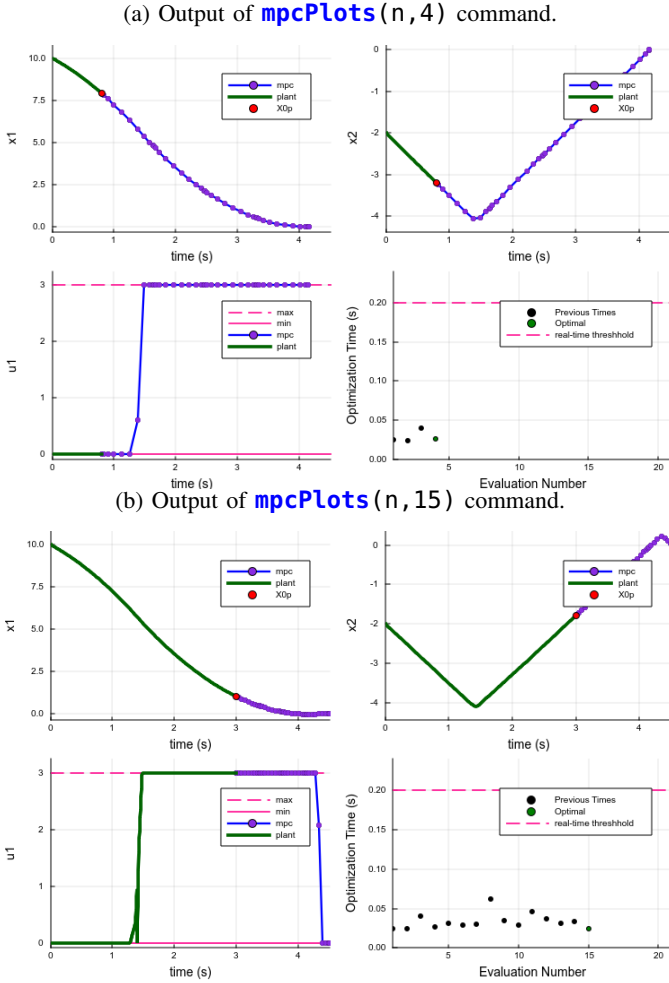


Fig. 4: Closed-loop visualization of moon lander problem using NLOptControl.

Direct methods are broken into shooting methods [61], multiple shooting methods [62], [63], and direct-collocation methods. Shooting methods are not suitable for most practical applications because they do not work well when the number of variables is large [64]. The multiple shooting method is well suited to exploit parallel processing due to the structure of its formulation [43], [65]. However, there are several disadvantages to the multiple shooting method: an expensive numerical integration needs to be performed during each iteration of the NLP solve, it can be difficult to incorporate state inequalities [64], and using multiple integration steps reduces the sparsity of the Hessian and Jacobian matrices [66]. Direct-collocation methods overcome these issues by enforcing the dynamic state constraints within the NLP. While this results in a larger problem, there is no need to perform expensive integrations of the state dynamics between iterations, because constraints in the NLP enforce the state dynamics at the collocation points, the path constraints can be easily incorporated, and the sparsity in the derivative matrices is preserved.

B. Direct-collocation method overview

Direct-collocation methods are divided into three categories of polynomial approximation types: h-methods (or local meth-

ods) [67], [68], [55], p-methods (or global methods) [69], [70], [71], and hp-methods (a hybrid of the h- and p-methods) [72], [1], [73]. In an h-method, the dynamic state constraints are satisfied using local approximations; e.g., Euler’s method or the trapezoidal method [67]. For h-methods, increasing the number and location of the collocation points [43], [1], [74] leads to convergence. However, a large number of points may be required for convergence, which can result in large solve-times [75]. p-methods can reduce the number of points needed for convergence, because they are more accurate than h-methods [76]. p-methods approximate OCPs using global polynomials constructed by collocating the dynamics at Gaussian quadrature points [76]. p-methods were originally developed to solve problems in computational fluid dynamics [77] and since have been used in practice in optimal control. For instance, p-methods were used to rotate the International Space Station 180 degrees without using any propellant² [70]. A drawback with p-methods is that the Jacobian and Hessian matrices are much denser than with h-methods, which results in a larger NLP [78].

By construction, hp-methods help to mitigate the accuracy issues with h-methods and the NLP problem size with p-methods. Instead of using a single polynomial as with p-methods, hp-methods use multiple polynomials constrained to be connected to one another at the endpoints. This construction reduces the size of the NLP while maintaining accurate approximations [73].

C. Direct-collocation methods in NLOptControl

At the time of this writing, three direct-collocation methods are implemented in NLOptControl: two h-methods and one p/hp-method. The remainder of this section illustrates how these methods are implemented in NLOptControl.

1) *h-Methods*: Euler’s backward method and the trapezoidal method are embedded in NLOptControl. However, before these h-methods are given, the h-discretization matrices used to approximate the continuous-time OCP are provided.

a) *h-Discretization Matrices*: Consider that t is sampled at N evenly spaced discretization points $\in [t_0 + t_{ex}, t_f]$ and denote the result as the vector $\mathbf{T} = [T_1, \dots, T_N]$. Then, for instance the $t_0 + t_{ex}$ and t_f are defined as T_1 and T_N , respectively. Denote the state and control discretization matrices as

$$x(t) \Big|_{t=\mathbf{T}} = \mathbf{X}$$

and

$$u(t) \Big|_{t=\mathbf{T}} = \mathbf{U},$$

respectively. $\mathbf{X}[i]$ is the state at the i^{th} collocation point; thus, $\mathbf{X}[1]$ and $\mathbf{X}[N]$ index the values of the initial and final states, respectively. The control matrix is similarly defined; $\mathbf{U}[i]$ is the control at the i^{th} collocation point. Denote the minimum and maximum discretized state limit matrices as

$$x_{min}(t) \Big|_{t=\mathbf{T}} = \mathbf{X}_{min}$$

²The cost of the fuel saved was estimated at one million dollars and control of the space station orientation was accomplished using gyroscopes [5].

and

$$x_{max}(t) \Big|_{t=\mathbf{T}} = \mathbf{X}_{max},$$

respectively. Similarly, the minimum and maximum control limit matrices are denoted as

$$u_{min}(t) \Big|_{t=\mathbf{T}} = \mathbf{U}_{min}$$

and

$$u_{max}(t) \Big|_{t=\mathbf{T}} = \mathbf{U}_{max},$$

respectively.

b) Euler's Backward Method: The dynamic constraints in Eqn. 5 are locally approximated at $(N - 1)$ points defined by $\mathbf{T}[2 : N]$. To accomplish this, $(N - 1) \times n_{st}$ implicit constraints are added as shown in Eqn. 17

$$\begin{aligned} \mathbf{0} &= \mathbf{X}[i + 1] - \mathbf{X}[i] - hF(\mathbf{X}[i + 1], \mathbf{U}[i + 1], \mathbf{T}[i + 1]) \\ &= \boldsymbol{\eta}_i, \text{ for } i \in (1 : N - 1) \end{aligned} \quad (17)$$

where h is the time-step size, which is determined by dividing the time span $(t_f - t_0 - t_{ex})$ by N .

The integral term in the cost functional in Eqn. 4 is approximated in Eqn. 18 as

$$I = h \sum_{i=1}^N L(\mathbf{X}[i], \mathbf{U}[i], T_i) \quad (18)$$

c) Trapezoidal Method: Similar to Euler's backward method, the dynamic constraints in Eqn. 5 are locally approximated at $(N - 1)$ points defined by $\mathbf{T}[2 : N]$. To accomplish this, the $(N - 1) \times n_{st}$ implicit constraints in Eqn. 19 are enforced with

$$\begin{aligned} \mathbf{0} &= \mathbf{X}[i + 1] - \mathbf{X}[i] - \frac{h}{2}(F(\mathbf{X}[i], \mathbf{U}[i], \mathbf{T}[i]) + \\ &F(\mathbf{X}[i + 1], \mathbf{U}[i + 1], \mathbf{T}[i + 1])) \\ &= \boldsymbol{\eta}_i, \text{ for } i \in (1 : N - 1) \end{aligned} \quad (19)$$

Next, the integral term in the cost functional in Eqn. 4 is approximated in Eqn. 20 as

$$I = \frac{h}{2} \sum_{i=1}^N (L(\mathbf{X}[i], \mathbf{U}[i], T_i) + L(\mathbf{X}[i + 1], \mathbf{U}[i + 1], T_{i+1})) \quad (20)$$

d) Discrete OCP: The h-method-based discrete OCP is given as

$$\underset{\mathbf{X}, \mathbf{U}, T_N}{\text{minimize}} \quad \mathcal{M}(\mathbf{X}[1], T_1, \mathbf{X}[N], T_N) + I \quad (21)$$

$$\text{subject to} \quad \boldsymbol{\eta} = \mathbf{0} \quad (22)$$

$$\mathbf{C}(\mathbf{X}, \mathbf{U}, \mathbf{T}) \leq \mathbf{0} \quad (23)$$

$$\boldsymbol{\phi}(\mathbf{X}[1], T_1, \mathbf{X}[N], T_N) = \mathbf{0} \quad (24)$$

$$\mathbf{X}_{min} \leq \mathbf{X} \leq \mathbf{X}_{max} \quad (25)$$

$$\mathbf{U}_{min} \leq \mathbf{U} \leq \mathbf{U}_{max} \quad (26)$$

$$t_{fmin} \leq T_N \leq t_{fmax} \quad (27)$$

where slack constraints can be included with the Mayer term in Eqn. 21 and Eqn. 23.

2) *p-Methods* : For generality, this paper only describes hp-methods, since the single interval method (i.e., p-method) is merely the case where the number of intervals is equal to one.

3) *hp-Methods* : The form of Eqn. 4 – Eqn. 11 must be modified to directly transcribe the OCP into an NLP using hp-methods. To apply Gaussian quadrature the interval of integration must be transformed from $[t_0 + t_{ex}, t_f]$ to $[-1, +1]$. To accomplish this, $\tau \in [-1, +1]$ is introduced as a new independent variable and a change of variable, for t in terms of τ using the affine transformation, $t = \frac{t_f - t_0 - t_{ex}}{2} \tau + \frac{t_f + t_0 + t_{ex}}{2}$. Then, the interval $\tau \in [-1, +1]$ is divided into a mesh of K intervals to accommodate for multiple intervals. With this, as in [75], an array of mesh points (M_0, \dots, M_K) for the boundaries of these intervals is defined, which satisfy

$$-1 = M_0 < M_1 < M_2 < \dots < M_{K-1} < M_K = 1$$

Denote the continuous-time variables for the state and control are on each mesh interval, $k \in (1, \dots, K)$, by the arrays $x^{(k)}(\tau)$ and $u^{(k)}(\tau)$, respectively. Next, denote arrays of continuous-time variables for both the minimum and maximum state and control limits on each mesh interval, $k \in (1, \dots, K)$, as $x_{min}^{(k)}$, $x_{max}^{(k)}$, $u_{min}^{(k)}$, and $u_{max}^{(k)}$, respectively. The state continuity between the mesh intervals is ensured with the constraint $x^{(k)}(M_k) = x^{(k+1)}(M_k)$ for $k = (1, \dots, K - 1)$ [73]. Similar to [1], this constraint is enforced programatically by making $x^{(k)}(M_k)$ be the same variable as $x^{(k+1)}(M_k)$. To continue to describe the hp-method implemented in `NLOptControl`, the hp-discretization matrices are defined, which hold the discrete-time values of the approximation to continuous-time problem.

a) hp-Discretization Matrices: First an array of time discretization vectors, $\boldsymbol{\tau}^{(k)} = [\tau_1^k, \dots, \tau_{N^k}^k]$, is defined by evaluating the continuous functions at N^k specified τ 's $\in [M_{k-1}, M_k]$ for $k \in [1, \dots, K]$, where N^k notates the number of collocation points in mesh interval k ; for instance, $\tau_1^1 = -1$. Let

$$\mathbf{N} = [N_1, N_2, \dots, N_k, \dots, N_{K-1}, N_K]$$

denote an array that holds the number of collocation points within each mesh interval, where N^k can be adjusted according to the desired level of fidelity for the k^{th} mesh interval. For $k \in [1, \dots, K]$, denote the state and control discretization matrix arrays as

$$x^{(k)}(\tau) \Big|_{\tau=\tau^{(k)}} = \mathbf{X}^{(k)}$$

and

$$u^{(k)}(\tau) \Big|_{\tau=\tau^{(k)}} = \mathbf{U}^{(k)},$$

respectively. Next, denote the minimum and maximum discretized state limit matrix arrays as

$$x_{min}^{(k)}(\tau) \Big|_{\tau=\tau^{(k)}} = \mathbf{X}_{min}^{(k)}$$

and

$$x_{max}^{(k)}(\tau) \Big|_{\tau=\tau^{(k)}} = \mathbf{X}_{max}^{(k)},$$

respectively. Similarly, the minimum and maximum control limit matrices are defined as

$$u_{min}^{(k)}(\tau) \Big|_{\tau=\tau^{(k)}} = \mathbf{U}_{min}^{(k)}$$

and

$$u_{max}^{(k)}(\tau) \Big|_{\tau=\tau^{(k)}} = \mathbf{U}_{max}^{(k)},$$

respectively.

To approximate the modified OCP that is modified for hp-methods, `NLOptControl` builds on the work done in [69], [79], [30], which was implemented in `GPOPS-ii` [1]. Specifically, `NLOptControl` implements the Legendre-Gauss-Radau quadrature collocation method (Radau collocation method). For completeness, this section will briefly describe this method, but for a more thorough explanation, the reader is referred to the seminal work done in [1], [69], [79], [30].

b) Radau Collocation Method: In hp-methods, the states are approximated within each mesh interval with a Lagrange polynomial as

$$x^{(k)}(\tau) \approx \sum_{j=1}^{N_k+1} \mathbf{X}[j]^{(k)} \mathcal{L}_j^{(k)}(\tau), \quad k \in [1, \dots, K] \quad (28)$$

with

$$\mathcal{L}_j^k(\tau) = \prod_{\substack{l=1 \\ l \neq j}}^{N_k+1} \frac{\tau - \tau_l^k}{\tau_j^k - \tau_l^k}, \quad k \in [1, \dots, K] \quad (29)$$

$\mathcal{L}_j^k(\tau)$ is the (k^{th}, j^{th}) Lagrange polynomial within a basis of Lagrange polynomials defined by $j = (1, \dots, N_k + 1)$ and $k = (1, \dots, K)$, $\boldsymbol{\tau}^{(k)} = [\tau_1^k, \dots, \tau_{N_k}^k]$ and is the k^{th} set of the LGR collocation points (also, called LGR nodes [80]), which are defined on the k^{th} mesh interval ($\tau \in [M_{k-1}, M_k]$). Then to approximate the entire state, M_k is added as a noncollocated point [69] for $k \in (1, \dots, K)$.

The derivative of the state can then be approximated for each mesh interval as

$$\frac{dx^{(k)}(\tau)}{d\tau} \approx \sum_{j=1}^{N_k+1} \mathbf{X}[j]^{(k)} \frac{d\mathcal{L}_j^{(k)}(\tau)}{d\tau}, \quad k \in [1, \dots, K] \quad (30)$$

with

$$\left. \frac{d\mathcal{L}_j^{(k)}(\tau)}{d\tau} \right|_{\tau=\tau_j^k} = D_{ij}^k \quad (31)$$

where D_{ij}^k is an element of the $N^k \times N^{k+1}$ Legendre-Gauss-Radau differentiation matrix in the k^{th} mesh interval, as defined in [69].

Next, in order to approximate the integral of the Lagrange term in Eqn. 4, Gaussian-Legendre quadrature [81] is used as

$$\int_{t_0+t_{ex}}^{t_f} L(x(t), u(t), t) dt \approx \frac{t_f - t_0 - t_{ex}}{2} \sum_{k=1}^K \sum_{j=1}^{N^k} \frac{M_k - M_{k-1}}{2} w_j^k L(\mathbf{X}[j]^{(k)}, \mathbf{U}[j]^{(k)}, \tau_j^k; t_0 + t_{ex}, t_f) \quad (32)$$

where $\mathbf{w}^{(k)} = [w_1^k, \dots, w_{N_k}^k]$ is the k^{th} array of LGR weights³.

Eqn. 32 is mathematically equivalent to the approximations made for the integral term in the cost functional in [73], but it is written in a slightly different form to reduce the computations needed within the NLP. Specifically, the $\frac{M_k - M_{k-1}}{2} w_j^k$ term is calculated outside of the NLP, for $j \in (1, \dots, N^k)$ and $k \in (1, \dots, K)$. The result is stored in an array of vectors. Thus, the design variable t_f is removed from the summations in `NLOptControl`.

c) Discrete OCP: The p-method-based discrete OCP is shown in Eqn. 33 - Eqn. 39 as

$$\underset{\mathbf{X}^{(k)}, \mathbf{U}^{(k)}, t_f}{\text{minimize}} \quad \mathcal{M}(\mathbf{X}[1]^{(1)}, t_0 + t_{ex}, \mathbf{X}[N_{K+1}]^{(K)}, t_K) + I \quad (33)$$

subject to

$$\sum_{j=1}^{N_k+1} \mathbf{X}_j^{(k)} D_{ij}^{(k)} - \frac{t_f - t_0 - t_{ex}}{2} \mathbf{f}(\mathbf{X}_i^{(k)}, \mathbf{U}_i^{(k)}, \tau_i^k; t_0 + t_{ex}, t_f) = \mathbf{0} \quad (34)$$

$$\mathbf{C}^{(k)}(\mathbf{X}[i]^{(k)}, \mathbf{U}[i]^{(k)}, \tau_i^k; t_0 + t_{ex}, t_f) \leq \mathbf{0} \quad (35)$$

$$\phi(\mathbf{X}[1]^{(1)}, t_0 + t_{ex}, \mathbf{X}[N_{K+1}]^{(K)}, t_f) = \mathbf{0} \quad (36)$$

$$\mathbf{X}[i]_{min}^{(k)} \leq \mathbf{X}[i]^{(k)} \leq \mathbf{X}[i]_{max}^{(k)} \quad (37)$$

$$\mathbf{U}[i]_{min}^{(k)} \leq \mathbf{U}[i]^{(k)} \leq \mathbf{U}[i]_{max}^{(k)} \quad (38)$$

$$t_{fmin} \leq t_f \leq t_{fmax} \quad (39)$$

for $(i = 1, \dots, N_k)$ and $(k = 1, \dots, K)$

4) Transforming to an NLP: Depending on the method, either the discrete OCP in Eqn. 21 - Eqn. 27 or the discrete OCP in Eqn. 33 - Eqn. 39 is then transformed into a large and sparse NLP given by Eqn. 1 - Eqn. 3.

Now that design and methods of `NLOptControl` have been provided, the following two sections compares its ease of use and speed to existing commonly used optimal control software.

V. EVALUATION DESCRIPTION

The next section compares `NLOptControl` and `PROPT` in terms of ease of use and speed. This section describes the conditions under which these comparisons are made.

A. Ease of use

Claiming that a software package is easy to use is subjective; even with the definition provided for ease of use, i.e., syntax that closely resembles the underlying OCP. Therefore, the respective syntax in `NLOptControl` and `PROPT` needed to model the moon lander OCP, as given in Eqn. 16, is compared.

B. Benchmark

The conditions under which `NLOptControl`'s speed is benchmarked against `PROPT` include the benchmark problem, methodology, and setup.

³To calculate both the LGR nodes and weights, `NLOptControl` leverages FastGaussQuadrature [82], [80], which uses methods developed in [83].

1) *Benchmark problem*: An OCP suitable for an NMPC-based ground vehicle application is used to benchmark `NLOptControl` against `PROPT`. The purpose of this problem is to find the steering and acceleration commands that drive a kinematic bicycle model [84], [85] to a goal location ($x_g = 0$ m, $y_g = 100$ m) as fast as possible (i.e., in minimum time) while avoiding crashing into a static obstacle. The cost functional is shown in Eqn. 40 as

$$\underset{\alpha_x(t), \alpha(t)}{\text{minimize}} \quad (x(t_f) - x_g)^2 + (y(t_f) - y_g)^2 + t_f \quad (40)$$

The dynamic constraints are shown in Eqn. 41 as

$$\begin{aligned} \dot{x}(t) &= u_x(t) \cos(\psi(t) + \beta(t)) \\ \dot{y}(t) &= u_x(t) \sin(\psi(t) + \beta(t)) \\ \dot{\psi}(t) &= \frac{u_x(t) \sin(\beta(t))}{l_b} \\ \dot{u}_x(t) &= a_x(t) \end{aligned} \quad (41)$$

where $x(t)$ and $y(t)$ are the position coordinates, $\psi(t)$ is the yaw angle, $u_x(t)$ is the longitudinal velocity, $\alpha(t)$ is the steering angle, $\beta(t) = \tan\left(\frac{l_a \tan(\alpha(t))}{l_a + l_b}\right)^{-1}$, $l_a = 1.58$ m and $l_b = 1.72$ m are the distances from the center of gravity to the front and rear axles, respectively. The path constraints ensure that the vehicle avoids an obstacle, these constraints are shown in Eqn. 42 as

$$1 < \left(\frac{x(t) - x_{obs}}{a_{obs} + m}\right)^2 + \left(\frac{y(t) - y_{obs}}{b_{obs} + m}\right)^2 \quad (42)$$

where $x_{obs} = 0$ m and $y_{obs} = 50$ m denote the position of the center of the obstacle, $a_{obs} = 5$ m and $b_{obs} = 5$ m denote the semi-major and semi-minor axes, $m = 2.5$ m is the safety margin that accounts for the footprint of the vehicle. The event constraints ensure that the vehicle starts at a particular initial condition, these constraints are given in Eqn. 42 as

$$\begin{aligned} x(t_0) &= 0 \text{ m}, & y(t_0) &= 0 \text{ m}, & \psi(t_0) &= \frac{\pi}{2} \text{ rad} \\ u_x(t_0) &= 15 \frac{\text{m}}{\text{s}}, & a_x(t_0) &= 0 \frac{\text{m}}{\text{s}^2}, & \alpha(t_0) &= 0 \text{ rad} \end{aligned} \quad (43)$$

That is the vehicle is traveling straight ahead at a constant velocity of $15 \frac{\text{m}}{\text{s}}$. The state and control bound constraints are given in Eqn. 44 as

$$\begin{aligned} -100 \text{ m} &\leq x(t) \leq 100 \text{ m}, & -0.01 \text{ m} &\leq y(t) \leq 120 \text{ m} \\ -2\pi \text{ rad} &\leq \psi(t) \leq 2\pi \text{ rad}, & 5 \frac{\text{m}}{\text{s}} &\leq u_x(t) \leq 29 \frac{\text{m}}{\text{s}} \\ -2 \frac{\text{m}}{\text{s}^2} &\leq a_x(t) \leq 2 \frac{\text{m}}{\text{s}^2}, & -\frac{30\pi}{180} \text{ rad} &\leq \alpha(t) \leq \frac{30\pi}{180} \text{ rad} \end{aligned} \quad (44)$$

The final time is constrained to be $0.001 \text{ s} \leq t_f \leq 50 \text{ s}$.

Solutions to Eqn. 40 - Eqn. 44 that are obtained in less than 0.5 s are deemed to be fast enough for real-time NMPC.

2) *Benchmark methodology*: Using the problem described above, a comprehensive benchmark is made between various solvers. A solver is defined by a particular combination of either `NLOptControl` or `PROPT` in conjunction with a particular direct-collocation method. The set of solvers S are listed in Table II as

TABLE II: Set of solvers tested

Legend label	Description
<code>NLOpt_{LGR1}</code>	<code>NLOptControl</code> with LGR nodes with a single interval
<code>NLOpt_{LGR2}</code>	<code>NLOptControl</code> with LGR nodes with two intervals
<code>NLOpt_{LGR4}</code>	<code>NLOptControl</code> with LGR nodes with four intervals
<code>NLOpt_E</code>	<code>NLOptControl</code> using Euler's method
<code>NLOpt_T</code>	<code>NLOptControl</code> using trapezoidal method
<code>PROPT_{C1}</code>	<code>PROPT</code> with Chebyshev nodes with a single phase
<code>PROPT_{C2}</code>	<code>PROPT</code> with Chebyshev nodes with two phases
<code>PROPT_{C4}</code>	<code>PROPT</code> with Chebyshev nodes with four phases

Comparisons between the average solve-times of single interval/phase solvers (i.e., `NLOptE`, `NLOptT`, `NLOptLGR2`, `PROPTC1`) and the multiple interval/phase solvers (i.e., `NLOptLGR2`, `NLOptLGR4`, `PROPTC2`, `PROPTC4`) must be considered in context. This is true because as the number of collocation points per interval/phase is increased, the two interval/phase solvers (i.e., `NLOptLGR2` and `PROPTC2`) and the four interval/phase solvers (i.e., `NLOptLGR4` and `PROPTC4`) are solving problems that roughly two and four times larger than the single interval/phase solvers, respectively. However, there are advantages of these multi interval/phase solvers, as discussed previously, that may be more important than the decreases in solve times. Thus, these solvers are included in the comparison here for a more comprehensive comparison.

Comparisons between the average solve-times of the multiple interval solvers in `NLOptControl` and the multiple phase solvers in `PROPT` also require consideration. Ideally, the benchmark between `PROPT` and `NLOptControl` would include the same direct-collocation methods. Unfortunately, `PROPT` and `NLOptControl` do not have the same direct-collocation methods. As such, comparisons are made between single/multiple phase Chebyshev pseudospectral methods in `PROPT` and multiple single/interval LGR pseudospectral methods in `NLOptControl`. Unlike a multiple interval method, in a multiple phase method, between phases, the constraints can change and the optimal transition time can be determined. In this work, the constraints do not change and the final time is divided evenly by the number of phases to determine the transition time. By doing this, the OCPs formulated by the multiple phase and multiple interval methods have roughly the same size and level of complexity. Thus, comparisons between the two software packages can be made with this issue in mind.

Each solver s is used to solve a set of problems P . The benchmark problem is discretized over the range of collocation points $p = 2, 3, \dots, 102$ per interval or phase to realize the set of problems P tested for each solver; a total of 101 different values of p (i.e., levels-of-fidelity or problems) are tested. Each test is performed three times to provide the data needed to calculate the average solve-time $t_{s,p}$ for the benchmark problem with a level-of-fidelity p using solver s . A polynomial is interpolated through the (x, y) solution points and sampled at 200 points to determine if the solution drives the vehicle through the obstacle. If a collision is determined for a particular combination of solver s^* and level-of-fidelity p^* , then t_{s^*,p^*} is set to NaN ; such solutions are not practically feasible.

Conducting many benchmark tests helps accurately rank the solvers. However, analyzing large sets of benchmark data

can be overwhelming and the conclusions drawn from such analyses can be subjective. To help eliminate these issues, this work uses an optimization software benchmarking tool called performance profiles [86].

Performance profiles show the distribution function for a particular performance metric. Here, the performance metric is the ratio of the solver’s average solve-time to the best average solver solve-time given as

$$r_{s,p} = \frac{t_{s,p}}{\min(t_{s,p} : s \in S)}$$

where this performance metric is calculated for each solver s at each level-of-fidelity $p = 2, 3, \dots, 102$. If a solver does not solve a particular problem, then $r_{s,p}$ is set to r_M . r_M is chosen to be a large positive number; the choice of r_M does not effect the evaluation [86].

To assess a solver’s overall performance on the set of problems, the cumulative distribution function for the performance ratio is defined as

$$\mathcal{P}_s(\Gamma) = \frac{1}{101} \text{size}(p \in P : r_{s,p} \leq \Gamma)$$

where $\mathcal{P}_s(\Gamma)$ is the probability that solver s can solve problem p within a factor Γ of the best ratio.

3) *Setup*: The setup is defined by the hardware platform and software stack. The results in this paper are produced using a single machine running Ubuntu 16.04 with the following hardware characteristics; an Intel Core i7 – 4910MQ CPU @2.90GHz \times 8, and 16GB of RAM. For software, both `NLOptControl` 0.1.5 and `PROPT` use `KNITRO` 10.3 for the NLP solver with the default settings, except the maximum solve-time, which is set to 300 s.

VI. RESULTS

A. Ease of use

Listing. 2 and Listing. 3 show the respective syntax in `NLOptControl` and `PROPT` needed to model the moon lander OCP in Eqn. 16. Section B in the Appendices shows `NLOptControl`’s and `PROPT`’s solutions compared to the analytical solution.

Listing 2: `NLOptControl` code needed to formulate and solve the moon lander problem. The `!` character indicates that the function is modifying the model.

```
n = define(numStates = 2, numControls = 1, X0
  ↪ = [10, -2], XF = [0., 0.], XL = [0,
  ↪ -20], XU = [20, 20], CL = [0.], CU=[3.])
  ↪ ;
2 dynamics!(n,[:(x2[j]), :(u1[j]) - 1.5]));
configure!(n;(:finalTimeDV => true));
4 obj = integrate!(n, :(u1[j]));
@NObjective(n.ocp.mdl, Min, obj);
6 optimize!(n);
```

`NLOptControl` can model OCPs more succinctly than `PROPT`. `NLOptControl` models Eqn. 16 with 5 lines of code, while it takes `PROPT` 12 lines — there are two main reasons for this: (1) it takes `PROPT` 4 lines of code to include the initial and final state conditions, and the upper and lower limits of the states and controls, while this is accomplished with a

single line of code, with `NLOptControl`, and (2) several of `PROPT`’s features are required, while in `NLOptControl` they are optional; these features include an initial guess, an options structure, and the naming of the state and control variables. Additionally, `PROPT` has more verbose syntax than `NLOptControl` — `PROPT`’s `collocate()`, `initial()`, and `final()` functions require many characters per line of code.

B. Speed

The performances of the solvers in Table II are now examined on the set of problems realized by various discretizations of Eqn. 40 – Eqn. 44, as described in Sec. V. The results for these examinations are in Fig. 5a and Fig. 5b. Fig. 5a shows the performance, or average solve-times $t_{s,p}$, for each solver s on each problem p . Fig. 5b shows the performance profiles for all of the solvers in four ranges of interest for Γ . Each range is on a separate plot. The purpose of this section is to (1) show the raw benchmark data in Fig. 5a and (2) provide an objective analysis of this data in Fig. 5b. In the following section, this information will be used to draw conclusions regarding the speed of `NLOptControl` and the best solver for the benchmark problem.

Fig. 5a shows that `NLOptControl`’s solvers are faster than `PROPT`’s. At a high-level, `NLOptControl` solves 88% of the problems in real-time using h-methods (i.e., `NLOptE` and `NLOptT`) and 46% of the time using p/hp-methods (i.e., `NLOptLGR2`, `NLOptLGR2`, and `NLOptLGR4`). `PROPT` only solves 0.05% of the problems in real-time using p/hp-methods (i.e., `PROPTC1`, `PROPTC2`, and `PROPTC4`). At a lower-level, the zoomed-in subplot in the the bottom graph of Fig. 5a shows that `NLOptControl` solves the benchmark problem in real-time when the number of collocation points per interval is less than: 80 for the single-interval case; 45 for the two-interval case; and 25 for the four-interval interval case. `PROPT` obtains real-time solutions when the number of collocation points per phase is less than 27 for the single-phase case and less than 4 for the two-phase case. For the four-phase case, `PROPT` cannot solve any of the problems in real-time.

Fig. 5a also shows that as the number of intervals/phases increase from `NLOptLGR1` to `NLOptLGR4` and `PROPTC1` to `PROPTC4`, the solve-times increase exponentially. Due to the large solve-times with `PROPT`’s solvers, these trends can only be seen in the top graph of Fig. 5a — the bottom graph shows the trends for `NLOptControl`’s solvers. As discussed in the previous section, this increase in solve time is largely due to the fact that with an increase in the intervals/phases larger problems are created and they take longer to solve. Even though the `NLOptLGR4` solver is solving a problem that is roughly four times larger than the `PROPTC1` solver, `NLOptLGR4` results in smaller solve-times.

Fig. 5a also shows that h-methods in `NLOptControl` are faster than the p-method for the benchmark problem. As the level-of-fidelity increases, the solve-times increase linearly with h-methods and exponentially with the p-method. Additionally, the number of collocation points needs to be greater than about 20 for the h-methods to ensure collision avoidance,

Listing 3: *PROPT* code needed to formulate and solve the moon lander problem

```

1 toms t t_f
2 p = tomPhase('p', t, 0, t_f, 30);
  setPhase(p);
4 tomStates x v
  tomControls a
6 cbox = {0.001<=t_f<=400, 0<=icollocate(x)<=20, -20<=icollocate(v)<= 20, 0<=collocate(a)<=3};
  ode = collocate({dot(x)==v, dot(v)==-1.5 + a});
8 cbnd = {initial(x == 10);initial(v == -2);final(x == 0);final(v == 0)};};
  x0 = {t_f == 1.5, icollocate({x == 0 v == 0}), collocate(a == 0)};
10 objective = integrate(a);
  options = struct;
12 prob = sym2prob(objective, {cbox, ode, cbnd}, x0, options);
  result = tomRun('knitro', prob, 1);

```

while the *p*-methods need 23 and 27 for `NLOptControl` and *PROPT*, respectively.

The four plots in Fig 5b show the ranges of Γ wherein certain solvers dominate. Each profile in this figure shows the probability \mathcal{P} that a given solver s will solve the set of problems P the fastest within a factor of Γ . At $\Gamma = 1$, the solver that has the highest probability of being the fastest is `NLOptE`, with a probability of 0.881. `NLOptE` dominates until about $\Gamma = 1.8$, at which point `NLOptT` has the highest probability of being the fastest, with a probability of 0.891. `NLOptT` dominates until about $\Gamma = 80$. The remaining approximate ranges of domination are as follows: `NLOptLGR2` from 80 to 160, `NLOptLGR4` from 160 to 5,000, *PROPT*_{C4} from 5,000 onwards. Given enough time, *PROPT*_{C4} solves 100% of the problems. For this benchmark problem, while the `NLOptT` and `NLOptE` solvers are much faster than the `NLOptLGR2`, `NLOptLGR4`, and *PROPT*_{C4} solvers they are not as reliable. However, the `NLOptT` and `NLOptE` solvers are both faster and more reliable than the `NLOptLGR2`, *PROPT*_{C1}, and *PROPT*_{C2} solvers.

VII. DISCUSSION

The approach detailed in Section II yields a direct-collocation-based optimal control modeling language that is both faster and easier to use than *PROPT*. The results and the following discussion support this claim.

`NLOptControl` is easier to use than *PROPT*, because its syntax is more concise, and focused on building a model of the OCP in Bolza form. Differences between Listing 2 and Listing 3, in terms of number of lines of code and the number of characters per line of code, indicate that `NLOptControl` models OCPs more succinctly than *PROPT*. This work speculates that *PROPT* requires more lines of code to formulate other more practical problems as well.

In addition to *PROPT*'s verbosity, its syntax is flexible to the extent that modeling errors are easier to be made. This claim is made because its users can more easily formulate problems that do not fit into the Bolza OCP form. As an example, consider using *PROPT* to model the dynamic constraints in Eqn. 5 for the moon lander problem — Line 7 in Listing 3. When using *PROPT*, if the user were to forget to include the second differential equation as

```
ode = collocate({dot(x)==v});
```

an error would not be displayed; such overly flexible syntax can lead to modeling errors. If that same mistake were attempted in `NLOptControl`, the user would be alerted as

```

julia> dynamics!(n,[:(x2[j])]);
ERROR: The number of differential equations
      ↪ must equal ocp.state.num.

```

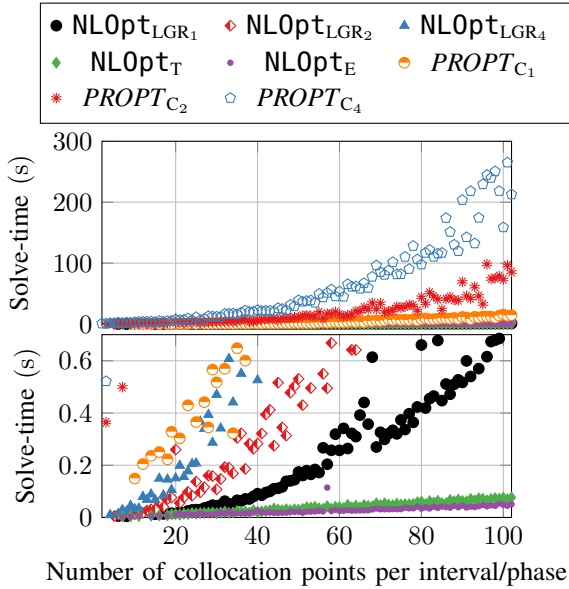
Thus, `NLOptControl` helps avoid modeling errors better than *PROPT*, because `NLOptControl`'s syntax does not allow users to formulate problems that are not in the Bolza form, while *PROPT*'s syntax does.

Both `NLOptControl` and *PROPT* can be used formulate OCPs, but *PROPT* takes a functional approach to this task rather than a modeling approach, as with `NLOptControl`. Listing 2 is compared to Listing 3 to support this claim. Listing 3 shows that, with *PROPT*, the user creates all of the components of the OCP and finally assembles them on Line 12. With `NLOptControl`, in Listing 2, it is clear from the first line of code that a model named `n` is being built. Using this approach, `NLOptControl` can clearly model and solve multiple OCPs at once. Such an object-oriented approach can further reduce potential modeling errors.

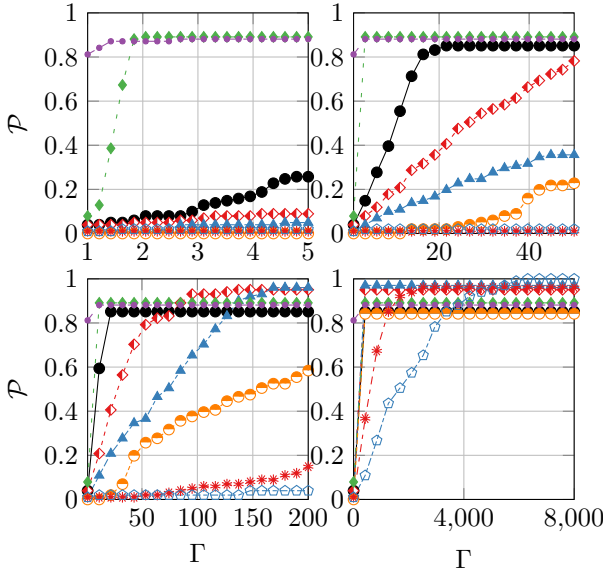
The benchmark results in Fig. 5a and Fig. 5b show that `NLOptControl` is faster than *PROPT*. Differences between these packages that affect speed include: differentiation methods, underlying computational language, and available direct-collocation methods.

PROPT uses symbolic automatic differentiation to calculate the derivatives. However, the structure of the Hessian matrices born from approximating an OCP using direct-collocation methods is sparse and symbolic automatic differentiation does not exploit this structure for speed. In contrast, `NLOptControl` uses the acrylic-coloring method to exploit the sparse structure of the Hessian matrix in conjunction with reverse automatic differentiation. Based on this difference, `NLOptControl` is expected to be faster than *PROPT*, especially when solving large problems that have a very sparse structure.

PROPT's differentiation methods are implemented in *MATLAB* and `NLOptControl`'s are implemented in *Julia*. Unfortunately, the literature does not contain benchmarks of



(a) The top graph shows all average solve-times obtained. The bottom graph shows the solve-times obtained near or below the real-time threshold of 0.5 s.



(b) Performance profiles: each graph shows the performance profiles for a different range of Γ .

Fig. 5: Benchmark results `NLOptControl` and `PROPT` for the kinematic bicycle problem, see Table II for legend explanation.

each of these differentiation methods in both *MATLAB* and *Julia*. However, research has shown that *Julia* is much faster than *MATLAB* for a wide range of problem types [33]. Thus, *Julia* may be able to run the reverse automatic differentiation method combined with the acrylic-coloring method to identify sparsity in the Hessian matrix faster than *MATLAB*—if it were implemented in *MATLAB*.

Overall, this paper speculates that `NLOptControl`'s unique combination of differentiation methods and computational language makes it faster than `PROPT`. This is only a speculation since the direct-collocation methods are different between `NLOptControl` and `PROPT`. However, the following pairs of solvers can be considered roughly equivalent in terms of their direct-collocation methods: `NLOpt_LGR1` and `PROPT_C1`, `NLOpt_LGR2` and `PROPT_C2`, and `NLOpt_LGR4` and `PROPT_C4`. Between these pairs, `NLOptControl` solves the problem roughly 14, 26, and 36 times faster than `PROPT`, respectively. It is unlikely that these large differences are due to either differences between collocating at Chebyshev nodes vs. LGR nodes, multiple interval vs. multiple phase methods, or some combination of the two. Thus `NLOptControl` is fast, which is especially important for MPC applications. A brief discussion of `NLOptControl`'s salient MPC functionality follows.

`NLOptControl` has optional functionality that helps account for the non-negligible solve-times in MPC applications. In MPC, often the control delay (i.e., solve-time) is neglected [19]. When the control delay is neglected, the current state of the plant is used to initialize the problem as opposed to initializing the problem with a prediction of what the plant's state will be after the solve-time has elapsed. Typically neglecting the solve-time in linear model predictive control is not an issue; because in linear MPC, the quadratic program is solved so quickly that initial state of the trajectory can be set to the current state of the plant without compromising robustness [87]. However, neglecting the solve-time in NMPC is likely to deteriorate robustness [88], because the NLPs often take a non-negligible amount of time to solve, after which the state of the plant will have evolved significantly. To make matters even more challenging, ensuring that the NLP solve-times are smaller than a particular execution horizon remains an unsolved problem [89], [90], [91], [87], [92], [93]. Fortunately, for many problems, these NLP solve-times are similar and an upper limit determined based on experience. This upper limit can be used to determine a fixed execution horizon. In `NLOptControl`, after the user selects an execution horizon, as described in Section. III, the framework in Fig. 3b can be used to account for non-negligible solve times. Frameworks such as this, can help establish conceptual schemes to improve safety and performance in NMPC applications.

VIII. CONCLUSIONS

This paper introduces an open-source, direct-collocation method based OCP modeling language called `NLOptControl`. `NLOptControl` extends the *JuMP* optimization modeling language to include a natural algebraic syntax for modeling OCPs. `NLOptControl` is compared

against *PROPT* in terms of ease of use and speed. *PROPT*'s syntax is shown to be more verbose and error-prone than *NLOptControl*'s; thus *NLOptControl* is easier to use than *PROPT*. This ease of use is largely attributed to *NLOptControl*'s use of the *JuMP* optimization modeling language. In addition to being easier to use, results from the benchmark tests show that *NLOptControl* is much faster than *PROPT*. *NLOptControl*'s superior performance is likely due to the unique utility of the *Julia* programming language and the reverse automatic differentiation method in conjunction with the acrylic-coloring method to exploit the sparsity of the Hessian matrices. *NLOptControl* emerges as an easy to use, fast, and open-source [9] optimal control modeling language that holds great potential for not only improving existing off-line and on-line control systems but also engendering a wide variety of new ones.

ACKNOWLEDGEMENTS

This work was supported by the Automotive Research Center (ARC) in accordance with Cooperative Agreement W56HZV-14-2-0001 U.S. Army Tank Automotive Research, Development and Engineering Center (TARDEC) Warren, MI. Benoît Legat provided a thoughtful review of this paper and discussions with the several *Julia* developers including Miles Lubin, Tony Kelman, and Chris Rackauckas were helpful.

REFERENCES

REFERENCES

- [1] M. A. Patterson, A. V. Rao, Gpops-ii: A matlab software for solving multiple-phase optimal control problems using hp-adaptive gaussian quadrature collocation methods and sparse nonlinear programming, *ACM Transactions on Mathematical Software (TOMS)* 41 (1) (2014) 1.
- [2] J. P. Sanchez, D. Garcia Yarnoz, Asteroid retrieval missions enabled by invariant manifold dynamics, *Acta Astronautica* 127 (2016) 667 – 677, asteroid mission;Easily retrievable objects;Libration point orbits;Low thrust;Trajectory designs; URL <http://dx.doi.org/10.1016/j.actaastro.2016.05.034>
- [3] M. M. E. Per E. Rutquist, *PROPT - Matlab Optimal Control Software*, Tomlab Optimization Inc., 1260 SE Bishop Blvd Ste E, Pullman, WA 99163, USA, 1st Edition (June 2016). URL https://tomopt.com/docs/TOMLAB_PROPT.pdf
- [4] T. Jorris, C. Schulz, F. Friedl, A. Rao, Constrained trajectory optimization using pseudospectral methods, in: *AIAA Atmospheric Flight Mechanics Conference and Exhibit*, 2008, p. 6218.
- [5] W. Kang, N. Bedrossian, Pseudospectral optimal control theory makes debut flight, saves nasa 1 m in under three hours (2007).
- [6] A. Holmqvist, F. Magnusson, Open-loop optimal control of batch chromatographic separation processes using direct collocation, *Journal of Process Control* 46 (2016) 55–74.
- [7] T. Utstumo, T. W. Berge, J. T. Gravdahl, Non-linear model predictive control for constrained robot navigation in row crops, in: *Industrial Technology (ICIT)*, 2015 IEEE International Conference on, IEEE, 2015, pp. 357–362.
- [8] J. V. Frasch, A. Gray, M. Zanon, H. J. Ferreau, S. Sager, F. Borrelli, M. Diehl, An auto-generated nonlinear mpc algorithm for real-time obstacle avoidance of ground vehicles, in: *European Control Conference, IEEE*, 2013, pp. 4136–4141.
- [9] H. Febbo, *NLOptControl*, <https://github.com/JuliaMPC/NLOptControl.jl> (2017).
- [10] A. V. Rao, D. A. Benson, C. Darby, M. A. Patterson, C. Francolin, I. Sanders, G. T. Huntington, Algorithm 902: Gpops, a matlab software for solving multiple-phase optimal control problems using the gauss pseudospectral method, *ACM Transactions on Mathematical Software (TOMS)* 37 (2) (2010) 22.

- [11] V. M. Becerra, Solving complex optimal control problems at no cost with psopt, in: *Computer-Aided Control System Design (CACSD)*, 2010 IEEE International Symposium on, IEEE, 2010, pp. 1391–1396.
- [12] M. Kelly, An introduction to trajectory optimization: How to do your own direct collocation, *SIAM Review* 59 (4) (2017) 849–904.
- [13] J. T. Betts, S. L. Campbell, N. Kalla, Initialization of direct transcription optimal control software, in: *Decision and Control, 2003. Proceedings. 42nd IEEE Conference on, Vol. 4, IEEE*, 2003, pp. 3802–3807.
- [14] A. V. Rao, User's manual for gpops c version 1.0: A matlab® implementation of the gauss pseudospectral method for solving multiple-phase optimal control problems (2007).
- [15] J. Andersson, J. Åkesson, M. Diehl, Casadi: A symbolic package for automatic differentiation and optimal control, in: *Recent Advances in Algorithmic Differentiation*, Springer, 2012, pp. 297–307.
- [16] I. M. Ross, A beginner's guide to dido: A matlab application package for solving optimal control problem, <http://www.elissar.ziz> (2007).
- [17] B. Ghannadi, N. Mehrabi, R. S. Razavian, J. McPhee, Nonlinear model predictive control of an upper extremity rehabilitation robot using a two-dimensional human-robot interaction model, in: *International Conference on Intelligent Robots and Systems, IEEE*, 2017, pp. 502–507.
- [18] G. Basset, Y. Xu, O. Yakimenko, Computing short-time aircraft maneuvers using direct methods, *Journal of Computer and Systems Sciences International* 49 (3) (2010) 481–513.
- [19] J. Liu, P. Jayakumar, J. L. Stein, T. Ersal, Combined speed and steering control in high-speed autonomous ground vehicles for obstacle avoidance using model predictive control, *IEEE Transactions on Vehicular Technology* 66 (10) (2017) 8746–8763.
- [20] H. Febbo, J. Liu, P. Jayakumar, J. L. Stein, T. Ersal, Moving obstacle avoidance for large, high-speed autonomous ground vehicles, in: *American Control Conference*, 2017, pp. 5568–5573.
- [21] B. Houska, H. J. Ferreau, M. Diehl, ACADO toolkit: An open-source framework for automatic control and dynamic optimization, *Optimal Control Applications and Methods* 32 (3) (2011) 298–312.
- [22] M. Lubin, I. Dunning, Computing in operations research using julia, *INFORMS Journal on Computing* 27 (2) (2015) 238–248. doi:10.1287/ijoc.2014.0623.
- [23] O. von Stryk, Dircol, Internet/WWW (2001).
- [24] . e. RWTH Aachen University, Germany, DyOS User Manual, 2002.
- [25] M. Diehl, D. B. Leineweber, A. A. Schäfer, *MUSCOD-II users' manual*, Universität Heidelberg. Interdisziplinäres Zentrum für Wissenschaftliches â€, 2001.
- [26] V. Leek, An optimal control toolbox for matlab based on casadi (2016).
- [27] R. H. Byrd, J. Nocedal, R. A. Waltz, Knitro: An integrated package for nonlinear optimization (2006).
- [28] L. T. B. Andreas Wachter, On the implementation of an interior-point filter line-search algorithm for large-scale nonlinear programming (2004).
- [29] P. E. Gill, W. Murray, M. A. Saunders, Snopt: An sqp algorithm for large-scale constrained optimization (2002).
- [30] M. A. Patterson, A. V. Rao, Exploiting sparsity in direct collocation pseudospectral methods for solving optimal control problems, *Journal of Spacecraft and Rockets* 49 (2) (2012) 364–377.
- [31] M. J. Tenny, J. B. Rawlings, R. Bindlish, Feasible real-time nonlinear model predictive control, in: *AICHE SYMPOSIUM SERIES*, New York; American Institute of Chemical Engineers; 1998, 2002, pp. 433–437.
- [32] A. H. Gebremedhin, F. Manne, A. Pothen, What color is your jacobian? graph coloring for computing derivatives, *SIAM review* 47 (4) (2005) 629–705.
- [33] J. Bezanson, S. Karpinski, V. B. Shah, A. Edelman, Julia: A fast dynamic language for technical computing, *arXiv preprint arXiv:1209.5145* (2012).
- [34] I. Dunning, J. Huchette, M. Lubin, Jump: A modeling language for mathematical optimization, *SIAM Review* 59 (2) (2017) 295–320. doi:10.1137/15M1020575.
- [35] A. Griewank, D. Juedes, J. Utke, Algorithm 755: Adol-c: a package for the automatic differentiation of algorithms written in c/c++, *ACM Transactions on Mathematical Software (TOMS)* 22 (2) (1996) 131–167.
- [36] J. Revels, Reversediff, <https://github.com/JuliaDiff/ReverseDiff.jl> (2017).
- [37] L. Lessard, X. Zhang, X. Zhu, An optimal control approach to sequential machine teaching, *arXiv preprint arXiv:1810.06175* (2018).
- [38] R. Fourer, On the evolution of optimization modeling systems, *Optimization Stories* (2012) 377–388.
- [39] R. E. Rosenthal, *Gams—a user's guide* (2004).
- [40] R. Fourer, D. Gay, B. Kernighan, *Ampl: A modeling language for mathematical programming*, 2002, Duxbury Press.

- [41] M. Udell, K. Mohan, D. Zeng, J. Hong, S. Diamond, S. Boyd, Convex optimization in julia, in: Proceedings of the 1st First Workshop for High Performance Technical Computing in Dynamic Languages, IEEE Press, 2014, pp. 18–28.
- [42] E. Fragniere, J. Gondzio, R. Sarkissian, J.-P. Vial, A structure-exploiting tool in algebraic modeling languages, *Management Science* 46 (8) (2000) 1145–1158.
- [43] J. T. Betts, *Practical methods for optimal control and estimation using nonlinear programming*, Vol. 19, Siam, 2010.
- [44] J. Huchette, M. Lubin, C. Petra, Parallel algebraic modeling for stochastic optimization, in: Proceedings of the 1st First Workshop for High Performance Technical Computing in Dynamic Languages, IEEE Press, 2014, pp. 29–35.
- [45] I. R. Dunning, *Advances in robust and adaptive optimization: algorithms, software, and insights*, Ph.D. thesis, Massachusetts Institute of Technology (2016).
- [46] M. Lubin, Y. Dvorkin, S. Backhaus, A robust approach to chance constrained optimal power flow with renewable generation, *IEEE Transactions on Power Systems* 31 (5) (2016) 3840–3849.
- [47] B. Legat, SumOfSquares, <https://github.com/JuliaOpt/SumOfSquares.jl> (2019).
- [48] A. H. Gebremedhin, A. Tarafdar, A. Pothen, A. Walther, Efficient computation of sparse hessians using coloring and automatic differentiation, *INFORMS Journal on Computing* 21 (2) (2009) 209–223.
- [49] J. Heinen, Gr, <https://github.com/jheinen/GR.jl> (2018).
- [50] E. F. M. D. John Hunter, Darren Dale, matplotlib, <https://github.com/matplotlib/matplotlib> (2018).
- [51] J. Meditch, On the problem of optimal thrust programming for a lunar soft landing, *IEEE Transactions on Automatic Control* 9 (4) (1964) 477–484.
- [52] P. O. Sokaert, J. B. Rawlings, Feasibility issues in linear model predictive control, *AIChE Journal* 45 (8) (1999) 1649–1659.
- [53] E. C. Kerrigan, J. M. Maciejowski, Soft constraints and exact penalty functions in model predictive control, in: UKACC International Conference, 2000.
- [54] C. Rackauckas, Q. Nie, Differentialequations.jl—a performant and feature-rich ecosystem for solving differential equations in julia, *Journal of Open Research Software* 5 (1) (2017).
- [55] J. T. Betts, Survey of numerical methods for trajectory optimization, *Journal of Guidance Control and Dynamics* 21 (2) (1998) 193–207.
- [56] L. T. Biegler, An overview of simultaneous strategies for dynamic optimization, *Chemical Engineering and Processing: Process Intensification* 46 (11) (2007) 1043–1053.
- [57] B. Paden, M. Čáp, S. Z. Yong, D. Yershov, E. Frazzoli, A survey of motion planning and control techniques for self-driving urban vehicles, *IEEE Transactions on Intelligent Vehicles* 1 (1) (2016) 33–55.
- [58] L. S. Pontryagin, *Mathematical theory of optimal processes*, CRC Press, 1987.
- [59] D. Garg, *Advances in global pseudospectral methods for optimal control*, Ph.D. thesis, University of Florida USA (2011).
- [60] D. G. Hull, Conversion of optimal control problems into parameter optimization problems, *Journal of Guidance, Control, and Dynamics* 20 (1) (1997) 57–60.
- [61] M. R. Osborne, On shooting methods for boundary value problems, *Journal of Mathematical Analysis and Applications* 27 (2) (1969) 417–433.
- [62] H. G. Bock, K.-J. Plitt, A multiple shooting algorithm for direct solution of optimal control problems, *IFAC Proceedings Volumes* 17 (2) (1984) 1603–1608.
- [63] M. Diehl, H. G. Bock, H. Diedam, P.-B. Wieber, Fast direct multiple shooting algorithms for optimal robot control, in: *Fast Motions in Biomechanics and Robotics*, Springer, 2006, pp. 65–93.
- [64] R. Sargent, *Optimal control*, *Journal of Computational and Applied Mathematics* 124 (1-2) (2000) 361–371.
- [65] M. Diehl, H. G. Bock, J. P. Schlöder, R. Findeisen, Z. Nagy, F. Allgöwer, Real-time optimization and nonlinear model predictive control of processes governed by differential-algebraic equations, *Journal of Process Control* 12 (4) (2002) 577–585.
- [66] J. T. Betts, W. P. Huffman, Exploiting sparsity in the direct transcription method for optimal control, *Computational Optimization and Applications* 14 (2) (1999) 179–201.
- [67] C. R. Hargraves, S. W. Paris, Direct trajectory optimization using nonlinear programming and collocation, *Journal of Guidance, Control, and Dynamics* 10 (4) (1987) 338–342.
- [68] W. W. Hager, Runge-kutta methods in optimal control and the transformed adjoint system, *Numerische Mathematik* 87 (2) (2000) 247–282.
- [69] D. Garg, M. Patterson, W. W. Hager, A. V. Rao, D. A. Benson, G. T. Huntington, A unified framework for the numerical solution of optimal control problems using pseudospectral methods, *Automatica* 46 (11) (2010) 1843–1851.
- [70] F. Fahroo, I. M. Ross, *Advances in pseudospectral methods for optimal control*, in: *AIAA Guidance, Navigation and Control Conference*, 2008, p. 7309.
- [71] G. Huntington, D. Benson, A. Rao, A comparison of accuracy and computational efficiency of three pseudospectral methods, in: *AIAA Guidance, Navigation and Control Conference*, 2007, p. 6405.
- [72] M. A. Patterson, W. W. Hager, A. V. Rao, A ph mesh refinement method for optimal control, *Optimal Control Applications and Methods* 36 (4) (2015) 398–421.
- [73] C. L. Darby, W. W. Hager, A. V. Rao, An hp-adaptive pseudospectral method for solving optimal control problems, *Optimal Control Applications and Methods* 32 (4) (2011) 476–502.
- [74] S. Jain, P. Tsiotras, Trajectory optimization using multiresolution techniques, *Journal of Guidance, Control, and Dynamics* 31 (5) (2008) 1424–1436.
- [75] C. L. Darby, A. V. Rao, A mesh refinement algorithm for solving optimal control problems using pseudospectral methods, *Proceedings of the AIAA* (2009).
- [76] G. Elnagar, M. A. Kazemi, M. Razzaghi, The pseudospectral legendre method for discretizing optimal control problems, *IEEE Transactions on Automatic Control* 40 (10) (1995) 1793–1796.
- [77] M. Y. Hussaini, T. A. Zang, Spectral methods in fluid dynamics, *Annual Review of Fluid Mechanics* 19 (1) (1987) 339–367.
- [78] C. L. Darby, *hp-Pseudospectral method for solving continuous-time nonlinear optimal control problems*, University of Florida, 2011.
- [79] D. Garg, W. W. Hager, A. V. Rao, Pseudospectral methods for solving infinite-horizon optimal control problems, *Automatica* 47 (4) (2011) 829–837.
- [80] M. Abramowitz, Stegun, *Handbook of Mathematical Functions* 55 (1965) 888.
- [81] C. F. Gauss, *Methodus nova integralium valores per approximationem inveniendi*, apud Henricvm Dieterich, 1815.
- [82] S. Olver, *Fastgaussquadrature*, <https://github.com/ajt60gaibb/FastGaussQuadrature.jl> (2017).
- [83] N. Hale, A. Townsend, Fast and accurate computation of gauss–legendre and gauss–jacobi quadrature nodes and weights, *SIAM Journal on Scientific Computing* 35 (2) (2013) A652–A674.
- [84] R. Rajamani, *Vehicle dynamics and control*, Springer Science and Business Media, 2011.
- [85] J. Gonzales, F. Zhang, K. Li, F. Borrelli, Autonomous drifting with onboard sensors, in: *Advanced Vehicle Control*, CRC Press, 2016, p. 133.
- [86] J. J. M. Elizabeth D. Dolan, *Benchmarking optimization software with performance profiles* (2001).
- [87] M. Diehl, H. J. Ferreau, N. Haverbeke, Efficient numerical methods for nonlinear mpc and moving horizon estimation, *Nonlinear Model Predictive Control* 384 (2009) 391–417.
- [88] L. L. Simon, Z. K. Nagy, K. Hungerbuehler, Swelling constrained control of an industrial batch reactor using a dedicated nmpc environment: Optcon, in: *Nonlinear Model Predictive Control*, Springer, 2009, pp. 531–539.
- [89] M. Morari, J. H. Lee, Model predictive control: past, present and future, *Computers & Chemical Engineering* 23 (4) (1999) 667–682.
- [90] A. Eskandarian, *Handbook of Intelligent Vehicles*, Springer, 2012.
- [91] T. Ohtsuka, K. Ozaki, Practical issues in nonlinear model predictive control: real-time optimization and systematic tuning, in: *Nonlinear Model Predictive Control*, Springer, 2009, pp. 447–460.
- [92] J. Albersmeyer, D. Beigel, C. Kirches, L. Wirsching, H. G. Bock, J. P. Schlöder, Fast nonlinear model predictive control with an application in automotive engineering, in: *Nonlinear Model Predictive Control*, Springer, 2009, pp. 471–480.
- [93] C. Kirches, L. Wirsching, S. Sager, H. G. Bock, Efficient numerics for nonlinear model predictive control, in: *Recent Advances in Optimization and its Applications in Engineering*, Springer, 2010, pp. 339–357.
- [94] H. Mirinejad, T. Inanc, An rbf collocation method for solving optimal control problems, *Robotics and Autonomous Systems* 87 (Supplement C) (2017) 219 – 225. doi:<https://doi.org/10.1016/j.robot.2016.10.015>. URL <http://www.sciencedirect.com/science/article/pii/S0921889015301639>

APPENDIX A
BRYSON-DENHAM PROBLEM

Fig. 6 shows the analytic solutions for the states, control, as well as costates compared to the results obtained with `NLOptControl` using a single interval with 30 LGR nodes. `NLOptControl` calculates these trajectories reasonably well.

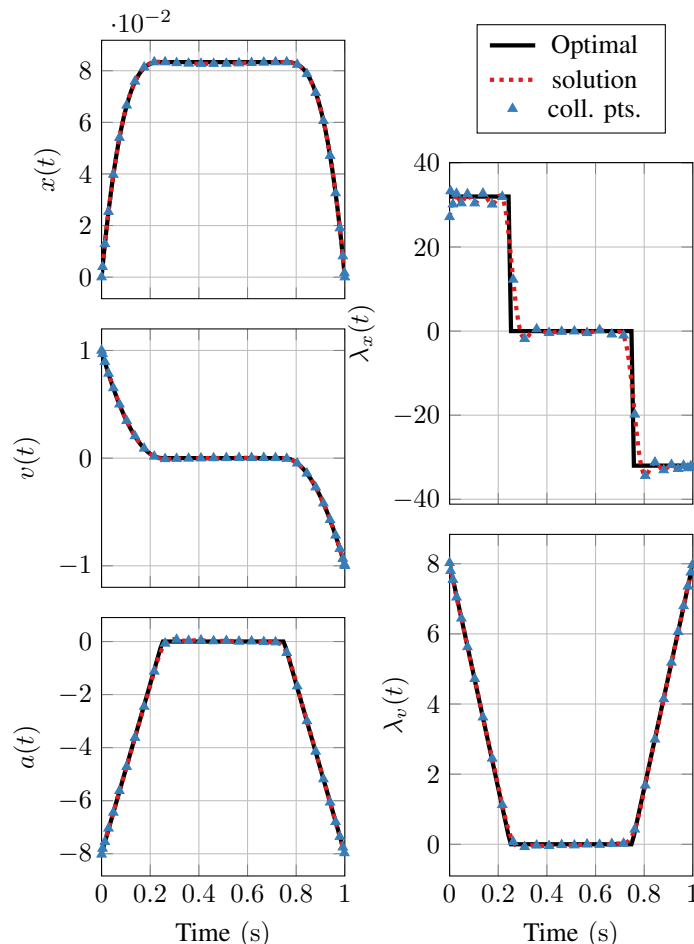


Fig. 6: State, control, and costate trajectories using `NLOptControl` (with 30 LGR nodes) compared to the analytical optimal solution for the Bryson Denham problem

The NLP solver for this example is *IPOPT* and an hp-method in `NLOptControl` is used with 4 intervals and 10 LGR nodes.

APPENDIX B
MOON LANDER PROBLEM

A. Closed-loop

Fig. 7 shows the closed-loop solution to the moon lander problem using `NLOptControl`. The closed-loop trajectory of the plant is very close to the analytic solution. Additionally, all of the solve-times are well below the chosen execution horizon t_{ex} of 0.2 s; thus `NLOptControl` solves this NMPC problem in real-time.

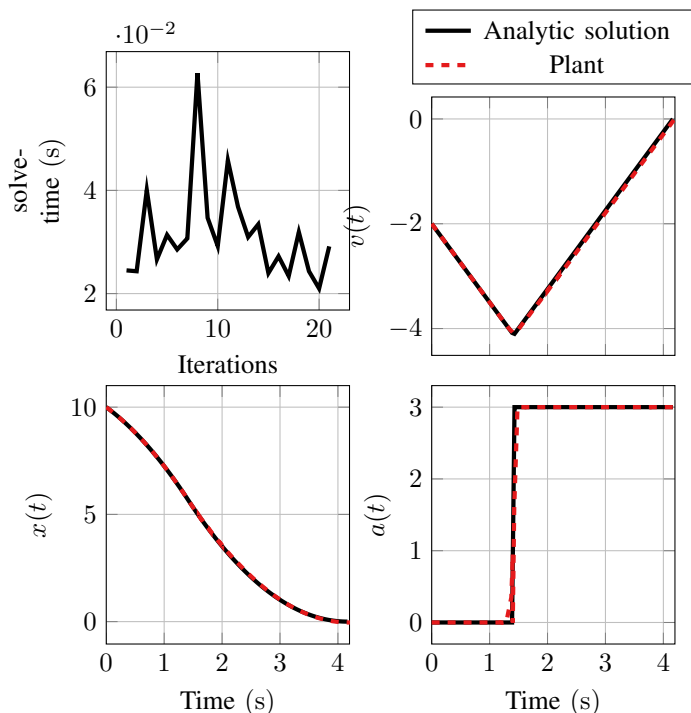


Fig. 7: Closed-loop trajectories for moon lander problem compared to the analytic solution

The NLP solver for this example is *IPOPT* and an hp-method in `NLOptControl` is used with 4 intervals and 10 LGR nodes.

B. Open-loop

In Fig. 8, it can be seen that both `NLOptControl` and *PROPT* determine the analytic solution accurately, with 30 LGR and Chebyshev nodes, respectively. However, there is an overshoot in the solution of the control with both `NLOptControl` and *PROPT*. This is due to the bang-bang nature of the analytic solution. It is noted that this overshoot may be mitigated using either mesh refinement [72], [75], [74] or radial basis functions [94].

APPENDIX C
BENCHMARK PROBLEM

This section provides an example of the type of solutions that are obtained from the benchmark between `NLOptControl` and *PROPT*. For `NLOptControl`, the hp-method with LGR nodes and four intervals and 10 collocation points per interval is used. *PROPT* is set to use four phases and 10 collocation points per phase and Chebyshev nodes. Fig. 9 compares the results of these solvers, where it can be seen that position trajectories are close. Starting at a speed of $15 \frac{m}{s}$, the solutions obtained from both *PROPT* and `NLOptControl` apply maximum acceleration from $t_0 = 0$ s to $t_f = 5.1$ s while avoiding collision with the obstacle and reaching the desired goal position. The trajectories for `NLOptControl` exhibit large oscillations in the α trajectory. These oscillations

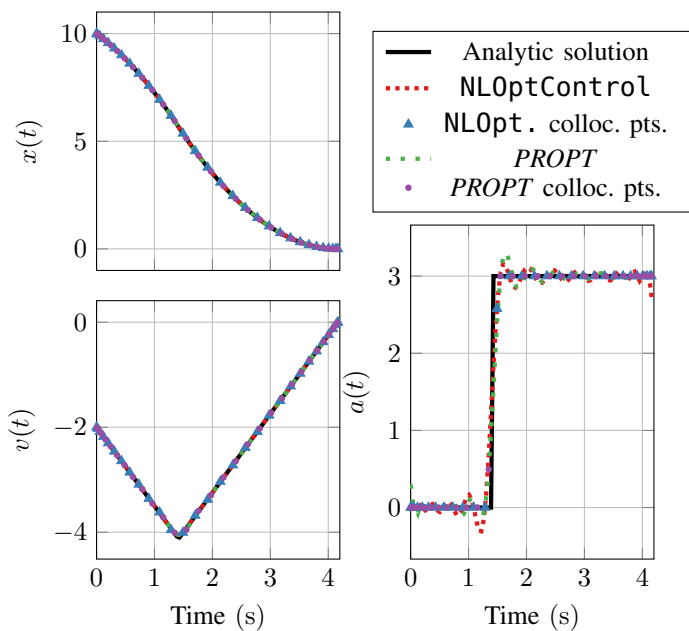


Fig. 8: State and control trajectories using `NLOptControl` (with 30 LGR nodes) and `PROPT` (with 30 Chebyshev nodes) compared to the analytic solution for moon lander problem

may be an artifact of the Runge phenomenon and seem to be reduced with `PROPT` as it uses Chebyshev nodes.

There is no analytic solution to this problem.

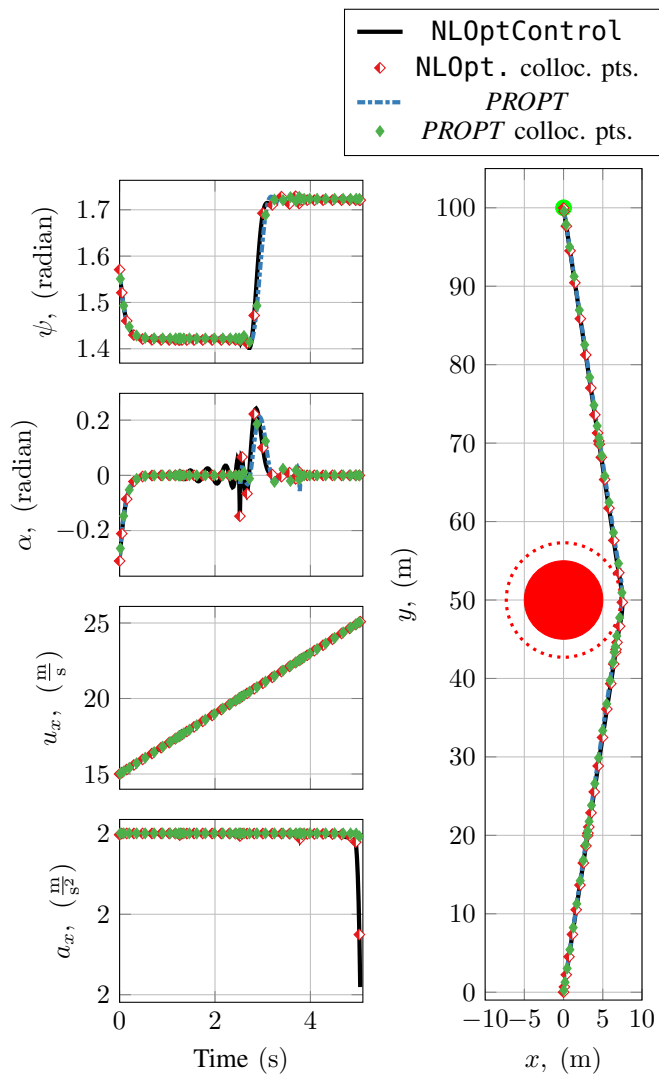


Fig. 9: State and control trajectories using `NLOptControl` (with 4 intervals and 10 LGR nodes) and `PROPT` (with 4 intervals and 10 Chebyshev nodes) for the kinematic ground vehicle problem